Effect of Urbanization on the Hyporheic Zone: Lessons from the Virginia Piedmont

Elizabeth Nadine Cranmer

Thesis submitted to the faculty of the Virginia Polytechnic Institute and State University in partial fulfillment of the requirements for the degree of

Master of Science
In
Environmental Engineering

Erich T. Hester
Glenn E. Moglen
Durelle T. Scott

June 28, 2011
Blacksburg, VA

Keywords: urbanization, stream, hyporheic, hydraulic conductivity, sediment

Effect of Urbanization on the Hyporheic Zone: Lessons from the Virginia Piedmont

Elizabeth Nadine Cranmer

ABSTRACT

As the world's population shifts toward living in cities, urbanization and its deleterious effects on the environment are a cause of increasing concern. The hyporheic zone is an important part of stream ecosystems, and here we focus on the effect of urbanization on the hyporheic zone from ten first-to-second-order streams within the Virginia Piedmont. We use sediment hydraulic conductivity and stream geomorphic complexity (vertical undulation of thalweg, channel sinuosity) as metrics of the potential for hyporheic exchange (hyporheic potential). Our results include bivariate plots that relate urbanization (e.g., total percent impervious) with hyporheic potential at several spatial scales. For example, at the watershed level, we observed a decrease in horizontal hydraulic conductivity with urbanization and an increase in vertical hydraulic conductivity, which ultimately results in a negligible trend from conflicting processes. Vertical geomorphic complexity increased with total percent impervious cover. This trend was somewhat unexpected and may be due to erosion of legacy sediment in stream banks. At the reach level, hydraulic conductivity increased and sinuosity decreased as the riparian buffer width increased; these trends are weak and are essentially negligible. The hydraulic conductivity results conform to expected trends and are a product of aforementioned concomitant processes. Our results emphasize the complexity of hydrologic and geomorphic processes occurring in urban stream systems at multiple scales. Overall, the watershed level effects enhancing hyporheic exchange, which is contrary to expectations. Given the importance of hyporheic exchange to stream function, further study is warranted to better understand the effects of urbanization.

Acknowledgements

The previous research would not be possible without several individuals. Dr. Cully Hession, Bethany Bezak, Laura Teany, and Denton Yoder provided access to the data from the Yagow et al. report (2008) and to some additional field equipment. Lei Jiang helped with the summer fieldwork, including the piezometer and permeameter installations, along with the thalweg surveying. Discussions with Dr. Erich Hester, Dr. Glenn Moglen, and Dr. Durelle Scott aided in the analysis of the data.

Table of Contents

List of Figures

List of Tables

1. Introduction

Urbanization is a global phenomenon, with population increasing in cities worldwide. This concentration of people puts a strain on water resources and the environment by increasing pollutant discharges and reducing the capacity of the environment to absorb and neutralize such pollutants. Another consequence of urbanization is the degradation and loss of habitat for organisms, both aquatic and terrestrial. Millions of dollars have gone to restoring streams (Bernhardt, et al., 2005; Palmer, et al., 2005) as societies recognize their importance for humans and ecosystems alike. Current restoration practice has created a new industry that attempts to create stable stream banks primarily for protecting human infrastructure (e.g., houses, roads, bridges). The industry's focus is generally on the stream's channel form, appeasing human aesthetics and assuming that ecological function will follow the stream form modifications (Kenwick, et al., 2009). In an effort to maximize the benefits of stream restoration, the fluvial connectivity to the hyporheic zone, a three-dimensional zone of interaction between groundwater and surface waters (Brunke & Gonser, 1997; Jones & Mulholland, 2000), has only recently been considered during restoration practices (Boulton, 2007; Kasahara, et al., 2009; Hester & Gooseff, 2010). Since the hyporheic zone contains flow paths that occur over several scales and is extremely heterogeneous, attempts to relate proxies of hyporheic extent and exchange to urbanization may benefit restoration practices.

1.1 Effects of Urbanization on Streams

Urbanization's effects on streams have been long documented. Since the 1950s, engineers have realized that urbanization increases flood peak discharges, decreases stream base flows, increases the volume of water transported in streams, degrades water quality, and makes streams flashy (Leopold, 1968; Whitlow & Gregory, 1989; Booth, et al., 2004; Mays, 2005).

Storm water management practices developed to deal with the increased peak flows, primarily through detention ponds designed to the retain peak discharge (Booth, et al., 2002; Mays, 2005).

Lane's work in 1955 indicated that sediment supply ($Q_{sediment}$) and discharge (Q_{water}) are in equilibrium with the median grain size (d_{50}) and channel slope ($S_{channel}$) in an undisturbed system (equation (1)).

$$Q_{sediment} \times d_{50} \propto Q_{water} \times S_{channel} \quad (1)$$

Changing the value of one parameter throws the system out of equilibrium. Using this relationship, some responses to urbanization can be predicted, especially with the use of Figure 1 (National Resources Conservation Service (NRCS), 2007). For example, urbanization increases Q_{water}, which can increase $Q_{sediment}$ and lead to channel degradation – a result commonly observed in streams (Graf, 1975; Booth & Jackson, 1997; Doyle, et al., 2000).

The effects of urbanization on fluvial geomorphology include changes to both stream geometry and the watershed drainage network. Stream sinuosity decreases as humans straighten streams and build within the floodplains, which can result in streams becoming disconnected from their floodplains (Lane, 1955; Chin, 2006; Notebaert, et al., 2011). Storm water management practices (culverts, etc.) can also increase drainage densities by artificially creating new streams and modifying existing ones (Walsh, et al., 2005; Chin, 2006).

Urbanization occurs in two phases, an initial intense construction phase and a long-term built-out phase. High sediment loads characterize the construction phase, with fines sediment depositing in the streams along with reductions in channel width (Graf, 1975; Chin, 2006). This sediment load eventually tapers off when construction ceases (Chin, 2006). The long-term built-out environment is characterized by increased impervious area, lower sediment loads than during construction (although often more than natural conditions), and decreased ecological health,

while the streams respond by widening the channel widths and incising (Wolman, 1967; Chin, 2006). The median grain size increases due to these changes as armoring and the flushing of fine sediment occurs (Wolman, 1967; Graf, 1975; Chin, 2006). This cumulative effect of multiple stressors is sometimes called the urban stream syndrome (Walsh, et al., 2005).

Various stream processes take different timescales to respond to urban stressors, primarily due to the complex relationship between the stream ecosystem and the land. For example, in gravel-bed streams, channel width and depth can take over a decade to respond, while streambed features, meander wavelengths, and reach gradients can take decades to centuries to reach equilibrium (Knighton, 1998). Antecedent conditions, such as legacy sediment stored behind historic low-head milldams (Walter & Merritts, 2008; Schenk & Hupp, 2009) blur the relationships between land use/cover and fluvial responses (Kang & Marston, 1993; Miller, et al., 1993; Colosimo & Wilcock, 2006; Horwitz, et al., 2008; Cuffney, et al., 2010). In particular, studies have found that sediment flushing times from the construction phase range from 5-13 years (Chin, 2006), while geomorphic change (adjustments to changing stream conditions from urbanization, climate, base-level change, etc.) can occurs over decades (Knighton, 1998; Chin, 2006). Furthermore, prior land use can have lingering effects. For example, Cuffney et al. (2010) found that in urbanizing watersheds that were once primarily agricultural, previous land use greatly influenced current stream condition. Similarly, a study by Miller et al. (1993) noted that land use changes during the 1940s and 1950s in Illinois led to decreased sediment supply that in combination with intense storm flows led to streams incision that was still occurring in the 1990s (Miller, et al., 1993). Kang & Marston (2006) found the greatest impact on sedimentation within urban streams to occur after 4-15 years but before 30 years. Regardless, stream discharge is not linearly correlated to drainage area (Galster, et al.,

2006). Thus, we would not expect urban stressors to linearly correlate with deleterious effects to streams.

Finally, urbanization itself is hard to measure. The most common method is total percent impervious area, which measures the fraction of the land that has impervious cover (e.g., pavement, rooftops). A key limitation of this metric is not all impervious area equally blocks infiltration to groundwater (Booth & Jackson, 1997). Specifically, connected impervious area (primarily roads and parking lots) more completely blocks infiltration than disconnected impervious area (some rooftops) by redirecting water to the storm water infrastructure, and is accordingly often the preferred metric (Schueler, 1994; Booth & Jackson, 1997; Wang, et al., 2001; Booth, et al., 2004; Roy & Shuster, 2009). An accurate assessment of connected impervious is difficult, requiring extensive field observations and storm water drainage system data (Roy & Shuster, 2009). Thus, some studies have tried to estimate connected impervious from total impervious area (Sutherland, 1995; Roy & Shuster, 2009) or developed land cover (Steedman, 1988; Wang, et al., 2001) although the relationships are often weak. Land cover, though informative, correlates less than connected impervious with ecosystem metrics (Wang, et al., 2001).

Previous studies have attempted to correlate total percent impervious with stream ecosystem health (Horwitz, et al., 2008; Cuffney, et al., 2010; Riva-Murray, et al., 2010), although most used a small range in urbanization or paired studies. In comparison, Clapcott et al. (2010) used a full urbanization gradient to look at land-use effects on stream health. A stream usually begins to show the deleterious effects of urbanization (e.g., reduction in water quality, reduced aquatic species diverseness) when its contributing watershed contains 3-10% impervious and is usually degraded above 15% (Schueler, 1994; Cuffney, et al., 2010). A very small

incremental change in the total impervious percentage can thus produce relatively large deleterious effects.

1.2 Hyporheic Zone and its Benefits

Channel bed forms (e.g., pools and riffles) and channel sinuosity generate head gradients that drive hyporheic flow in streams (Boano, et al., 2006; Gooseff, et al., 2006). Mixing of surface water with deeper groundwater in the hyporheic zone creates unique conditions that facilitate stream temperature buffering, biogeochemical cycling, and pollutant mitigation, while creating habitat (Brunke & Gonser, 1997; Boulton, et al., 1998; Dent, et al., 2000; Groffman, et al., 2005). Many organisms spend all or part of their life cycles within the hyporheic zone (Wood & Armitage, 1997; Boulton, 2007). The inherent heterogeneity of hyporheic sediments and flow paths along with the unique chemical environments – predominately from oxygen and carbon sources from surface water and high interstitial surface area of sediments – create redox gradients within sediments. The redox gradients, in turn, cause biogeochemical hot spots (Kasahara & Hill, 2008), which can be important for the life of the stream (Brunke & Gonser, 1997). The wide range of redox conditions are conducive to a wide range of reactions, including denitrification, mineralization of organic toxins, and precipitation of metals (Conant, et al., 2004; Fischer, et al., 2005; Gandy, et al., 2007; Smith, et al., 2009).

1.3 Expected Impact of Urbanization on Hyporheic Potential

Human activity affects hyporheic exchange and function in streams in a variety of ways (Hancock, 2002; Hester & Gooseff, 2010). In this study, we quantify those impacts in terms of their effect on hyporheic exchange via Darcy's law. In particular, an increase in hydraulic conductivity (K_h and K_v horizontally and vertically, respectively) increases water exchange in Darcy's Law, $Q = AKi$ (Todd & Mays, 2005), while an increase in stream geomorphic complexity (sinuosity S horizontally (Cardenas, 2009) and vertical complexity (VC) of the

thalweg (Hester & Doyle, 2008) increases the hydraulic gradient, *i*. All these metrics we collectively define as hyporheic potential.

Based on existing literature, we expect the following responses of hyporheic potential to urbanization at two spatial viewpoints – the watershed and reach levels (Figure 2). These represent our hypotheses that we aim to test. The watershed level viewpoint encompasses the watershed upstream of the field site and focuses on land cover-driven processes (i.e. upstream processes influencing the stream reach) (Richards, et al., 1996; Wang, et al., 2001). The reach level viewpoint focuses on the riparian buffer immediately adjacent to the stream reach of interest, lateral inputs/constraints, and direct impacts to channels (Allen, et al., 1997; Wang, et al., 2001; Cianfrani, et al., 2006). We discuss the anticipated response of each metric of hyporheic potential to urbanization in detail below. Note that the trends in Figure 2 are shown as linear not because we expect linear trends per se, but because we choose to form expectations only about direction of trends rather than trend shape, and linear is used as the simplest default.

1.3.1 Response to Urbanization at Watershed Level

We expect an increase in connected impervious (or developed land cover) within a watershed to increase input of fine sediments to streams and therefore colmation (clogging of pore spaces (Brunke, 1999; Packman & MacKay, 2003; Velickovic, 2005; Fries & Taghon, 2010)) of the streambed during and for a while after the construction phase. Fine sediments can come from anywhere within the watershed (Schueler, 1994; Richards, et al., 1996): a study from the UK showed that fine sediments can be transported up to 30 km downstream and penetrate unconsolidated streambed sediments as deep as 60 cm (Petts, 1988), though the effects are greatest near the source. Improper sedimentation control activities and road construction are key contributors (Carter, et al., 2003; Chin, 2006). During the construction phase, we therefore

expect increases in percent urban land cover or impervious area to be associated with decreased *K*.

On the other hand, during the built-out development phase, an increase in connected impervious may lead to two conflicting effects on *K***:** a decrease because of colmation from fine sediments from stream bank erosion and an increase from streambed coarsening during bed erosion. During the built-out scenario, fine sediment can erode from various locations within the channel system during the increased peak storm discharges of urban watersheds. For example, 2/3 of the sediment supply to the channel can come from stream banks (Trimble, 1997), which is often silt, clay and fine sands in the Piedmont of the Mid-Atlantic (Wolman, 1954). Similar fine sediment is also stored behind shallow-head, valley-wide milldams from earlier agricultural periods (Walter & Merritts, 2008; Cranmer E., 2009; Merritts, et al., 2011). In contrast, where stream banks are more stable, fine sediments are not eroded, allowing elevated urban storm flows to remove fine sediment from the streambed thereby coarsening shallow sediments (armoring) (Chin, 2006). This flushing of fines (Rheg, et al., 2005) could theoretically reverse colmation during the built-out phase and increase *K*. Observed results then reflect a combination of current urbanization and past land uses, instead of just urbanization.

We expect an increase in connected impervious area at the watershed level to decrease *VC*. Urbanization leads to larger runoff volumes and higher peak storm flows, which causes channel degradation. Other observed results include armoring of sediments in incised channels and upstream erosion causing downstream aggradation. This instability decreases *VC*, even to the loss of pool-riffle sequences (Schueler, 1994; Doyle, et al., 2000; Walsh, et al., 2005). Urbanization can therefore homogenize the streambed through sedimentation and/or the removal of natural hydraulic structures.

Lane's balance predicts that as connected impervious area increases, *S* should increase all else equal. By increasing the water supply and decreasing the sediment supply during built out conditions, the stream may respond through decreasing the upstream slope through increasing *S*. This assumes no channelization or encroachment by urban infrastructure and little influence of bank stability or vegetative cover (see section 1.3.2 for details).

1.3.2 Response to Urbanization at Reach Level

Possible metrics of urbanization at the reach level (within the riparian buffer) include percent urban land cover and total percent impervious within the riparian buffer, proximity of roads, and width of forested riparian buffer. For this study, we chose riparian-forested buffer width because we felt it had the most physical basis and has been shown to correlate with commonly used biotic indices (Allen, et al., 1997; Brabec, et al., 2002). We consider that decreasing forested buffer widths are indicative of increasing urbanization.

We expect that greater forested buffer widths are indicative of vegetated banks, which ultimately increases *K*. The increase in *K* comes from the vegetation stabilizing the banks, and thereby decreasing bank erosion (Allmendinger, et al., 2005; Pollen & Simon, 2005). The decrease in bank erosion means less fine sediments are entering the stream and undergoing colmation, assuming that the stream banks are mostly comprised of fine sediments. Healthy, mature riparian corridors aid in limiting fine sediment transport from the riparian buffer (Fullerton, et al., 2006).

We expect that streams with larger forested buffer widths should have greater *VC*. One cause was discussed previously: larger buffers reduce sediment input to the channel by reducing bank erosion – sediment inputs that would otherwise reduce vertical complexity by filling in pools. Wider buffers potentially also yield a greater source of large wood to the stream channel, thereby increasing *VC*. On the other hand, reduced bank erosion may also reduce the large wood

recruitment that bank retreat could cause, thereby reducing the increasing in *VC* that might otherwise occur due to increased supply of large wood to the channel.

We expect to find narrower buffers associated with decreased *S* due to past channelization for flood control, navigation, property boundary marking, or other purposes (Pizzuto, et al., 2000; Walsh, et al., 2005; Chin, 2006). A case study from Zimbabwe shows how the sinuosity of marshy land disappeared entirely as its channels were straightened (Whitlow & Gregory, 1989).

1.3.3 Goals of Current Study

While some studies of the hyporheic zone have been conducted within urban watersheds (Ryan & Boufadel, 2007; Ryan, et al., 2010), we are aware of none that evaluate our hypotheses across a full range of urbanization. This study is a first-attempt at understanding urbanization's effect on the hyporheic zone through hyporheic potential, specifically through *K*, *S*, and *VC*. A graphic summary of our expected trends is included as Figure 2.

2. Methods

2.1 Study Sites

We selected our study sites from among those of a larger study of 50 watersheds in the Virginia piedmont and coastal plain near Richmond and Fredericksburg VA and Washington DC (Yagow, et al., 2008). Of the 50 sites, we selected ten piedmont locations (Table 1, Figure 3) to span a broad range of urbanization, minimize variation in stream order and parent geology, and to eliminate agricultural land cover.

2.2 Reach Level Characterization of Hyporheic Potential

At each site, we selected a stream reach approximately 300 m in length for sinuosity analysis and a subset approximately 100 m in length at the center of the 300m reach for thalweg surveying and falling head tests. The 300 m and 100 m reaches were selected such that the sinuosity analyses and thalweg surveys were reasonably representative of the larger stream system by containing several meanders and pool-riffle sequences, respectively. We surveyed the thalweg of the 100 m sections with an autolevel and stadia rod, taking measurements every few meters and at all sharp discontinuities in the streambed such as large wood and steps. Some of the thalweg surveys were less than 100 m due to major obstructions (i.e. large trees that we were unable to move around). The stream sinuosity was calculated by first digitizing the 300 m reach stream banks from the aerial photos (Virginia Base Mapping Program (VBMP), 2006) in ArcGIS and then measuring both the thalweg length and the linear (down valley) length of the reach. Following a similar method to Gooseff et al. (2007), *S* was used as the metric for horizontal complexity, while *VC* was calculated as the root mean square of the difference of each survey point elevation from the linear trendline of the whole thalweg survey (equation (2))

$$VC = \sqrt{\sum_{i=1}^{n}(y_i - s_i)^2/n} \qquad (2)$$

where s_i is the relative streambed elevation at a given point *i* (meters), y_i is the calculated streambed elevation from the linear trendline at point *i* (meters), and n is the total number of surveyed points.

We used reusable permeameters and piezometers to measure K_v and K_h, respectively. The permeameters were constructed in a similar manner to Genereux et al. (2008). We marked clear polycarbonate tubing (inner diameter = 6.985 cm, outer diameter = 7.620 cm) every 0.5 cm with a permanent marker. The piezometers were also made from the polycarbonate tubing (inner diameter = 3.175 cm, wall thickness = 0.3175 cm) to which we added a nylon drive point. The lowest 5 cm of the piezometer were reserved for sediment collection, while the next 10 cm were for the screened interval. In the screened area, we drilled holes with a 0.476 cm (3/16 inch) bit, and then covered the section with tautly stretched drain-sock material secured by electrical tape. We marked the sediment/water interface at ten cm above the top of the screen section, and subsequently marked the piezometer every 0.5 cm thereafter with a permanent marker.

All permeameters and piezometers were developed using a Geotech peristaltic pump after each installation and prior to falling head tests. Falling head tests (Horslev, 1951; Kalbus, et al., 2006) were conducted by filling the tube with water to the top and then letting water levels return to background. Onset Hobo pressure transducers (model # U20-001-04) recorded the water pressure at the bottom of the water column in the tube (bottom of the piezometer and at the sediment surface in the permeameter, respectively). The logging interval was ten seconds for the permeameters and one second for the piezometers because water levels dropped faster in the piezometers. The pressure transducers were cooled in stream water for ten minutes before use to maintain data quality. For each field site, we conducted 8-12 permeameter tests and 3-10 piezometer tests. Sediment coarseness prevented piezometer installation in certain locations, as

the screened section of the piezometer was not completely covered because the piezometer could not be fully inserted 25 cm into the streambed, which is a necessary requirement for the falling head tests.

We used a time series of pressures generated during the falling head piezometer and permeameter tests to calculate K_h and K_v, respectively. The Hobos recorded pressures, which then were converted to pressure heads. For the piezometers (K_h), we calculated the percent recovery of the pressure heads and plotted them against time on a semi-log plot. The percent recovery of the heads can be calculated by

$$\frac{h-H}{H_0-H} \tag{3}$$

where h is the head at any point in time (meters), H is the head at the sediment-water interface (meters), and H_0 is the head when the piezometer is completely full (meters). According to Horslev (1951), the time lag, T_0, occurs when the percent recovery is 37% on the semi-log plot and K_h is equivalent to

$$K_h = \frac{R^2 \ln(L/R)}{2LT_o} \tag{4}$$

where R is the radius of the piezometer tubing (meters) and L is the screened linear length of the screened interval (meters).

For the permeameters (K_v), the Darcy method, equation (5), uses the change in head to calculate K_v (Landon, et al., 2001).

$$K_v = \frac{L_v \ln(H_0/H_f)}{(T_f-T_0)} \tag{5}$$

L_v is the length of permeameter within the streambed (meters), H_0 is the initial head (meters), T_0 is the initial time (seconds), H_f is the final head (meters), and T_f is the final time (seconds). In this method of calculation, the final time can be at any point (Landon, et al., 2001); some studies

have used regressions to generate this time value (Chen, 2000; Genereux, et al., 2008; Chen, et al., 2009). By contrast, the Horslev method – following Genereux et al. (2008) – requires an anisotropy ratio in order to complete the calculation – a value that cannot be known aprioi. Some simplifications exist that are dependent on the diameter size and depth of penetration into the bed sediments (Song, et al., 2010) – but these conditions were not satisfied in this study. We calculated K_v by using both methods and found that the result was almost identical; thus, we used the Darcy simplification for our remaining calculations.

Reach-wide representative K_h and K_v's were calculated as the geometric mean of all measurements within the reach. We digitized the location of each piezometer and permeameter in ArcGIS on the 2006 aerial photography (VBMP, 2006). We noted geomorphic feature type for every location we took a K measurement. We defined riffles as shallower, steeper, and higher velocity sections typically with coarser sediment, while the slower, deeper sections with lower velocities were considered pools (Montgomery & Buffington, 1997). Stream sections that were not classified as pools or riffles were considered runs. We also calculated geometric mean K for each geomorphic feature type. For both K_h and K_v, we also conducted an analysis of variance (ANOVA) statistical test at α=.05 to compare the variance within each field site to variance among field sites.

2.3 Watershed Level Characterization of Urbanization

We used the watershed delineations that Yagow et al. (2008) created from the National Elevation Dataset (NED) using Spatial Analyst in ArcGIS. We calculated the percent urban/developed land cover within each watershed from the Normalized Land Cover Dataset (NLCD) Center (Vogelmann, et al., 2001; Homer, et al., 2004) and land cover datasets from Coastal Change Analysis Program by the National Oceanic and Atmospheric Administration

(NOAA) (NOAA Coastal Change Analysis Program). Both datasets use 30 m by 30 m pixels and determine their land cover parameters from satellite imagery. The NOAA land cover dataset differs from the NLCD in that the NOAA datasets include more detailed wetland land cover types. The NLCD datasets (1992, 2001, and 2006) did not include the detailed wetland land cover types and cannot be directly compared to each other because of the reclassification of land cover types (Fry, et al., 2009). Unlike the 1992 NLCD product (which only produced a land cover product), three additional datasets are associated with the 2001 NLCD – a total percent impervious dataset, a percent canopy cover dataset, and the change in land cover between the two time periods (i.e. the difference between the percent impervious values for the two years, also known as a change product). At time of press, the 2006 NLCD dataset is provisional and includes the total percent impervious and change in percent impervious from 2006 to 2001. For our analysis, we used two urbanization metrics – percent total impervious and percent developed land cover – that were averages from each watershed. The impervious dataset came from the 2006 NLCD total percent impervious provisional data, which contained pixels with percentages of imperviousness. The land cover came from the 2005 NOAA land cover dataset; the urbanization metric was the percentage of that total area that was classified as developed land cover.

We also calculated the rate of change of urbanization over time. For the NOAA land cover datasets, NOAA developed an ArcGIS tool that calculates total percent impervious for the entire watershed by using their land cover dataset and population data along with curve numbers. The change in land cover was then calculated from the NOAA data by using the difference between two different datasets. For the NLCD data, the 2006-2001 change product for total imperviousness was used. For both NOAA and NLCD, the resulting rates of change used in the

analysis are absolute differences in land cover and total imperviousness, respectively, rather than percent changes in those variables.

2.4 Reach Level Characterization of Urbanization

We characterized riparian zone urbanization via forested buffer width. We first digitized the 300 m stream reaches and riparian forest extent on both sides of the stream was digitized from the aerial photography. The riparian width was then determined by dividing the forested area by twice the reach length to arrive at an average buffer width for a single side of the stream. We also calculated the buffer widths for the 100 m reaches for comparison. Since there was little difference in the values calculated for the different reach lengths, as well as the conclusions that we derived from them, we chose to only carry one buffer width estimate (300 m) forward in the analysis.

2.5 Bivariate Plot Analysis

We used bivariate plots to analyze the response of hyporheic potential to urbanization metrics. Many such plots are possible, so in our analysis we focused on a subset of possible plots with preference for relationships that 1) have greater statistical significance (higher r^2), 2) were expected based on physical processes as discussed in the introduction, and 3) use total percent impervious as the urbanization metric due to its greater physical meaning. We analyzed the relationships via a best-fit linear regression. In certain cases we also qualitatively evaluated trends in the maximum envelope, i.e. a trend in the upper bound of the points in the scatter plot e.g., Wang et al. (2001), particularly when linear regression r^2 values were low and such an interpretation made physical sense.

3. Results

Figures 4 through 7, 12 through 17, 19, 20, and 22 through 29 show the surveyed thalwegs for the stream reaches and the locations of the *K* measurements. Field sites P4 and P10 had particular trouble with piezometer installations due to streambed coarseness, while P12 has a low number of measurements due to the low water level within the stream (P12 looked more like a series of disconnected pools than a flowing stream). Field photos (Figures 8 through 11, 18, 21, 30, and 31) are included to help clarify certain features in the stream, and are further discussed in Section 3.3. Table 2 shows the reach-averaged *K* values, along with the other hyporheic potential metrics.

3.1 Response to Watershed-Level Urbanization

K_h decreases with increasing impervious cover and increasing urban land cover (Figure 32, both r^2 <.01). On the other hand, K_v indicated an increase with increased impervious cover and increased developed land cover (Figure 33, respectively r^2 <0.01 & r^2 =0.04). Nevertheless, both the K_h and K_v trends are negligible. K_h and K_v similarly decrease and increase, respectively, with increasing rate of change in the NLCD total percent impervious between 2001 and 2006 (Figure 34, respectively r^2 =0.01 & r^2 =0.06). Again, the regression trends are negligible. Similar to the regression trends the maximum K_h and K_v for a given degree of urbanization (maximum envelope K_h and maximum envelope K_h, respectively) decrease and increase, respectively with the change in urbanization. Nevertheless, both the regression trend and maximum envelope trend for K_v are heavily dependent on P19's values; if P19 is removed, both trends are reversed. *VC* increases as impervious cover and urban land cover increase (Figure 35, respectively r^2 =0.15 & r^2 =0.19), while a similar trend exists for *S* (Figure 36, respectively r^2 =0.38 & r^2 =0.15).

3.2 Response to Reach-Level Urbanization

K_h and K_v appear to increase with increasing riparian buffer width (Figure 37, respectively r^2 =0.02 & r^2 =0.12). *VC* and *S* decrease with increasing forested buffer widths (Figures 38 & 39, both respectively r^2 =0.09). Nevertheless, all reach-level trends are negligible or nearly negligible. Several studies have suggested that the effectiveness of riparian buffer widths in mitigating urban-derived stressors begin to decrease at around 100 to 150 m (Allen, et al., 1997; Brabec, et al., 2002). Based on this and the fact that our buffer widths were all less than 150 m, none of the field sites was eliminated from the resulting plots.

3.3 K Heterogeneity within Field Reaches

The ten field sites have a range of streambed conditions from fine sediment to small boulders. The streams are predominately gravel-bed streams. The streambeds of P1 and P2 appear to contain moderately sized clasts (large sands & small gravels). P5, P8, P9, and P12's streambeds are slightly finer than P1& P2's. The streambed of P4 and P6 ranges from silts and fine sands to buried boulders (riprap fallen into the stream), but the dominate clast size is gravels. P10's streambed appears to be mostly comprised of cobbles, while P19's streambed appears to be very fine gravels. Since grain size analysis of the streambed was not conducted, any conclusions drawn about the clast size come from visual analysis and hence are qualitative.

K varies within each field site. We placed most of the piezometers and permeameters within the thalweg, with about 17% off to one side. The piezometers off to one side were moved away from the thalweg due to streambed coarseness in the thalweg that prevented the screen section from being fully covered. The permeameters encountered difficulties in similar places and were moved off to one side due to stability issues. We also tried to cover a range of streambed features (pools, riffles, etc.) in order to generate an average *K* that was representative of the whole reach. *K* measurements for P12 were in pools due to the lack of surface water

elsewhere in the reach. The aerial photograph figures show the individual measurements along with their spatial distribution (Figures 5, 7, 13, 15, 17, 20, 23, 25, 27, & 29). Field sites with the smallest range of measurements tend to come from streams with visually more homogenous streambed distributions, i.e. P1 and P19 (Figure 40). The ANOVA showed that K_h did not vary among field sites at the .05 significance level ($F_{(9,67)} = 1.648$, $p = 0.120$). On the other hand K_v did vary significantly ($F_{(9,82)} = 8.378$, $p < 0.001$), but this result is dependent on only one significantly different site (P19). Variation among sites for both K_h and K_v is therefore minimal to negligible, consistent with the low r^2 values in Figures 32, 33, and 37. The variation in K within sites is therefore often as large or larger as variation among site means, particularly for K_h.

Given the aforementioned variability within the streams, three narratives describe some of the range in conditions. Sites P2 and P8 highlight some of the differences between highly urban and less urban streams. Site P19 is unique in that it has a highly urban watershed, yet has a well-sorted very fine gravel streambed. P2 is a predominately gravel stream within a highly urban (22.5% impervious 2006 NLCD, 75.29% urban land cover NOAA) watershed near McLean, VA. This field site is located in a local park with single-family housing on either side of the park. The stream is migrating, cutting into the stream bank, and exposing a clay/silt layer (Figure 8). Human trash, such as styrofoam and plastic trash bins, litters the stream (Figure 9). Fallen trees partially block sections of the stream flow (Figure 10). In the summer of 2010, one local resident observed that larger clasts were beginning to dominate the streambed.

Gravels dominate P8, a tributary to Cedar Run in Prince William County VA. This watershed is the second most pristine of all the field sites (0.1% impervious 2006 NLCD, 0.58% urban land cover NOAA). The watershed contains large residential lots, which from satellite

imagery results in the land cover being classified as forest. Orlando Road crosses over the tributary (Figure 21).

P19, Beaver Branch, is a well-sorted, very fine gravel stream near Richmond, VA in Henrico County and contains large amounts of urbanization (21.0% impervious 2006 NLCD, 71.07% urban land cover NOAA).The field site is located within a park. East of the park there is residential housing, while west of the park there are commercial buildings. Two culverts drain the commercial area's parking lots into this stream reach, while two storm water structures have been exposed (Figures 30 and 31). The locals call the very fine gravel stream bank their "beach" and allow children to play on the banks and in shallower sections of the stream.

4. Discussion

4.1 Response to Watershed-Level Urbanization

We expected that as urbanization increases in the contributing watershed, *VC* decreases, *S* increases, and the effect on *K* depends on the net effect of several competing processes (Section 1.3). *K* should decrease as a function of change in urbanization. The actual results showed that *VC* unexpectedly increased, while *S* increased as expected (Figure 41). The trends for K_h and K_v were essentially negligible. Due to the high level of scatter in our plots, which is typical of relationships between urban metrics and stream ecosystem metrics (Clapcott, et al., 2010), we used a cutoff of r^2=0.15 to distinguish between negligible and non-negligible trends.

Elevated levels of fine sediments come from both phases of urbanization (Chin, 2006). The initial phase of urbanization dumps extremely large loads of watershed-derived sediment into the streams (Schueler, 1994; Richards, et al., 1996), especially through improper sedimentation controls (Carter, et al., 2003). The built-out phase sees a slightly elevated level of fine sediment (two to five times higher than background concentration) when compared with natural conditions. The primary source of sediment during build-out is from stream bank erosion (Booth & Jackson, 1997; Trimble, 1997). As mentioned in the introduction, urbanization often leads to channel incision, which aids in altering streambed features. These multiple sources of fine sediment may explain some of the observed variability in *K* within and among sites (Figure 40).

The somewhat elevated level of fine sediments undergoing colmation and the general increase in streambed coarseness (through either armoring or the preferential removal of fines from the streambed (Chin, 2006)) may balance each other to produce the negligible trends observed (Figures 32-33). Furthermore, colmation could be reversed through resuspension of

sediments or bioturbation by benthic macroinvertebrates (Nogaro, et al., 2006). In particular, K_v might be more affected than K_h if burrows are mostly vertical, potentially explaining the slight difference in trends observed. Another possibility is fine sediment accumulations at depths deeper than those sampled by the permeameters. In particular, fine sediment particle size can influence the settling velocity and the depth of penetration within the streambed (Rehg, et al., 2005). A flume study by Schälchli showed that the depth of colmation, d_c, can be estimated by the mean streambed grain size, d_m, when measured in meters (Brunke, 1999; Velickovic, 2005).

$$d_c = 3d_m + 0.1\ m \quad (6)$$

For gravel (2-64 mm), the depth of colmation ranges from 10.6 to 29.2 cm. If the permeameters were measuring conductivity above such a deeper colmation depth, it would be possible for the K_v to increase at the same time that K_h decreases with increased urbanization – especially if the streams are still responding to the combination of urbanization and past land uses instead of just urbanization. Finally, increased peak storm discharge with increased urbanization could coarsen the bed due to preferential erosion of fines from the bed and banks (Chin, 2006) and ultimately out-compete with the colmation process. Regardless, both trends were sufficiently weak suggesting that it is important not to over-interpret its meaning.

The trends of K_h and K_v versus rate of change in total percent impervious between 2001 and 2006 were essentially negligible (Figure 34). The range of the change in percent impervious among our study watersheds (0.1-4.7%) is small compared to the overall range of imperviousness (0.1-47.3%). This low rate of change is likely due to many our watersheds being located in the northern part of the state (i.e. Fairfax County), where rapid urbanization occurred between 1950-1970s (Banham, 2009; Hogan & Walbridge, 2009). The higher observed percentages tended to come from field sites outside of Fairfax County. The low rate of change

indicates that sediment from new construction probably does not have a large effect on our study streams, which is consistent with the negligible trends. In addition, some of the scatter in the plots is likely due to a temporal mismatch between the impervious data (2001 & 2006) and the *K* data (2010).

The unexpected increase in *VC* with increased urbanization in theory could be explained by from localized adjustments to downed trees. Urbanization typically erodes stream banks by undercutting, especially if the tree roots along the bank do not reach the toe of the bank (Pollen & Simon, 2005; Allmendinger, et al., 2005). Undercut stream banks can topple these trees securing the bank (Pizzuto, et al., 2010) and this wood supply can then increase prevalence of geomorphic forms such as pools. Legacy sediment is prevalent within the Mid-Atlantic Piedmont (Walter & Merritts, 2008; Pizzuto & O'Neal, 2009), and is mostly comprised of pre-Colonial upland soils deposited behind millpond dams. These deposits can add upwards of a meter onto the pre-Colonial land surface (Cranmer E. , 2009), increasing the stream bank height and exacerbating bank erosion. The addition of large woody debris (LWD) competes with homogenization of the streambed through deposition of sediment from upstream or bank erosion. Given the observed trend, addition of LWD may at first appear the best explanation, yet the streams with the highest *VC* (P1, P2, P5, & P6) are not those with the largest number of fallen logs (P4, P6, & P8); instead, the observed LWD frequency seems to be uncorrelated with *VC*.

The increase in *S* with increased urban land cover is consistent with the Lane's Balance prediction. As urbanization increases, stream discharge increases and sediment supply decreases. To return to equilibrium, the stream needs to decrease the channel slope by increasing the channel sinuosity. Given that the streams in our study are relatively unconstrained for urban environments (forested buffer widths of 27 to 145 m; average is 66 m), this explanation is quite

plausible. The meander wavelengths can take several years to centuries to geomorphically resolve (Knighton, 1998), but most of the development in the watersheds used for this study is sufficiently old.

4.2 Response to Reach-Level Urbanization

As buffer width increases (i.e. local encroachment of urbanization decreases), we expect K_h, K_v, *VC*, and *S* to all increase (Section 1.3). Our results for *K* conform to the predicted trends, but *S* and *VC* decreased with larger buffer widths (Figures 37-39). However, these trends are sufficiently weak as to be negligible (Figure 41). This lack of significant trends may have individual causes specific to particular metrics of hyporheic potential (in particular for *VC* which we discuss here in Section 4.2), or instead it may mean that forested buffers do not have a significant influence on hyporheic potential (which we feel is more likely – see Section 4.4).

Unexpectedly, *VC* decreased with larger buffer widths (Figure 38). In theory, the stabilizing effect of more vegetation in wider buffers should reduce sediment inputs to the channel that would otherwise fill in pools, thereby increasing *VC*. Similarly, larger riparian buffers may provide a larger source of LWD to the channel, which could increase *VC*. On the other hand, as discussed previously, narrower buffers could lead to increased stream bank erosion which instead adds *greater* amounts of large wood to the stream channel through undercutting the stream banks (Pizzuto, et al., 2010). The net effect of these processes could explain the lack of observed trend. Nevertheless, the small amounts of LWD present in the field sites mentioned earlier makes this unlikely.

4.3 Heterogeneity within Sites & by Geomorphic Feature

Sediment *K* varies widely, especially among different streambed features and clast sizes. We present figures showing the location and approximate value of each measurement (Figures 8 through 11, 18, 21, 30, and 31).The ANOVA analysis indicates that the variability within each

field site is greater than among the field sites, except for P19's K_v. This is corroborated the large spread in standard deviations for each field site (Figure 40). This is reasonable given the small sample size (Table 2) and the inherent natural variability in streambed K (Calver, 2001), particularly since we intentionally spanned a range of geomorphic conditions (pools, riffles, runs). Nevertheless, we determined mean values for each geomorphic feature type (Table 3). We qualitatively defined riffles as shallow, fast-moving sections of the stream with coarser clasts, and pools as deep, slow-moving sections with fine sediment. Stream sections that were not classified as riffles or pools were classified as runs. We expect riffles to have higher hydraulic conductivities due to steeper slopes and faster moving water (UK Environmental Agency, 2009). The measured mean K values do not seem to support this expectation (Table 3). Again, the small sample size and inherent K variability can explain some of the results. Another possibility for the variability could come from the qualitative method of distinguishing geomorphic feature types. Lastly, the depths of the sediments characterized by the falling head tests (~10-20 cm) may somehow have been inappropriate for detecting the differences of interest. The changes in the streambed grain size, local flow conditions, and local weather would also further complicate the comparison among geomorphic features. Given all these variations, we provide narratives of three individual sites (P19, P2, and P8) that are useful in explaining some of the heterogeneity.

P19 was often the outlier in our plots. Unlike the other field sites that tended to have poorly sorted mixture of clasts from fines to boulders, P19 appears to have well sorted clasts that are predominately very fine gravel. This well sorted property (i.e. tending to have the same grain size) seems to explain why K_v at P19 is an order of magnitude larger than the other streams (Table 3). Besides P19's dominant grain size, the physical presence of two sewer manholes (Figure 31) makes the stream unique.

We now use P2 (highly urban) and P8 (relatively pristine) to contrast the effect of urbanization within a stream reach. The fallen trees in P2 disrupt the stream flow (Figure 10) and often generate pools (Figure 11). Since pools tend to develop on bends from the scour from helical flow paths, surviving tree roots on the banks help deepen these pools by diverting the water from the bank toward the streambed (Gran & Paola, 2001). P8's banks are much shorter, giving the vegetation a better chance of stabilizing the banks and reducing erosion (Figure 20). Field observations at P8 do not show obvious signs of erosion, while locals' testimony at P2 indicate that bank erosion is occurring in addition to the coarsening of the streambed clasts. At P2, three possible sediment sources of the larger clasts exist. Firstly, the clasts could come from a general consequence of urbanization and the higher peak discharge it generates. Secondly, the interstate highway construction in the upper sections of the watershed could be adding larger clasts to the stream reach. Lastly, the clasts could be transported from the melt-water from the three winter storms of the 2009-2010 season (each with over a foot of snow accumulation). The dominant process most likely is the higher peak discharge, as it preferentially erodes the finer sediments and leaves the coarse ones behind (Chin, 2006). Heterogeneity within reaches appears to have more sources and interactions in an urbanized watershed as opposed to a rural one.

4.4 Implications of Urbanization for Hyporheic Potential and Extent

Stream studies show that ecosystem metrics (e.g., LWD counts, riparian shade cover, taxa richness) weakly correlate with urbanization metrics (Cianfrani, et al., 2006; Clapcott, et al., 2010; Cuffney, et al., 2010) and that a high degree of noise is inherent. Most of our correlations are similarly very weak ($r^2 < 0.15$), indicating urbanization generally has weak or conflicting effects on hyporheic potential. In fact, one overall conclusion is that reach-scale urbanization (forested buffer width in the case of this study) has essentially no effect on hyporheic potential

(Figure 41). Control on hyporheic potential is therefore scale dependent, with watershed-level processes being more important than reach-level processes. Furthermore, both reach-level and watershed-level urbanization appear to have negligible effect on *K*, perhaps because bank erosion and streambed coarsening balance each other.

Nevertheless, we did observe two trends where r^2 was greater than 0.15 that we feel are probably significant given the noisiness inherent in this type of study. In particular, *VC* and *S* both increased with watershed-level urbanization (Figure 41), indicating that urbanization enhances hyporheic potential at the watershed level and (given no net effect at the reach-level) more generally. This overall conclusion is unexpected in that hyporheic exchange is generally considered as positive for stream ecosystems as well as for humans via ecosystem services, and we generally expect urbanization to degrade stream ecosystem function.

This study measured hyporheic potential as *K*, *S*, and *VC*. Additional measurements would expand the picture of urban impacts on hyporheic exchange. For example, salt tracer studies (Harvey & Bencala, 1993; Briggs, et al., 2010) can provide direct integrated reach-level measurements of exchange to compare to hyporheic potential used in this study. Conducting pebble counts or sieve analyses could help interpret the *K* results by quantifying the range of clast sizes and approximating the depth of colmation.

The highly complex relationship between urban streams and their watersheds, and the great number of processes and variables that affect urban streams, contribute heavily to the scatter observed in our results (Clapcott et al., 2010). Since the field sites came from the Yagow et al. (2008) study, the bedrock geology, stream size, and stream slope were partially controlled. Nevertheless, remaining variation in stream size and slope could influence *K* and *VC* and hence hyporheic exchange. If this study was repeated with new or additional watersheds, minimizing

these variations might reduce observed scatter. Furthermore, variation among watersheds in terms of storm water infrastructure or best management practices (BMPs, e.g., sediment control plans during construction and detention ponds during built out conditions) were ignored in our GIS analysis and could contribute to scatter. These controls could be incorporated in the future based on aerial photographs or ground surveys. BMP density could also be estimated based on building ages (estimated from housing styles[1]) and historical trends in BMPs in Fairfax County. In particular, storm water detention ponds were not prevalent in Northern Virginia until the late 1970s. Adding the storm water infrastructure to the analysis would better predict the actual sediment delivery and timing from the watershed to the stream reaches and could help interpret or refine the bivariate plots. Finally, clearer relationships might be obtained by determining connected impervious (as opposed to total impervious used in this study) for each watershed because it is a better predictor of urbanization effects than total impervious because it has more direct physical impacts on stream health (Roy & Shuster, 2009).

[1] My father's comments on building trends within Northern Virginia can be used as field estimate of the age of the development. Houses built in the 1950s contain brick facades, windows on all sides for cross-ventilation, and high-pitched roofs. Houses built in the 1960s tend to have carports. Houses from the 1970s will have siding on all except one facade, enclosed garages, and be multi-stories (split-level or two stories); houses in the 1980s and later look like bigger versions of 1970s housing. (Cranmer M. , 2010)

5. Conclusion

Urbanization and its associated impacts disrupt the dynamic equilibrium of streams, changing their physical condition, and degrading stream ecosystems. The hyporheic zone is an integral part of streams, is often important to ecosystem function, and can potentially remediate pollutants. It is therefore logical to expect that urbanization degrades hyporheic exchange and function, yet this has not been studied quantitatively. This study attempted to do so by examining how hyporheic potential metrics (i.e. proxies for hyporheic exchange: sediment hydraulic conductivity (K) and stream complexity (VC and S)) vary along an urbanization gradient in the Virginia piedmont.

Results at the watershed level indicate that in the watersheds we studied, increased urbanization as percent developed land cover and total percent impervious, is associated with essentially no changes in K_h and K_v, and increased VC, & S (Figure 41). While many potential mechanisms may be behind the observed trends, increased fine sedimentation from stream bank erosion and streambed coarsening at higher urbanization may cancel, thereby creating an overall negligible trend for K. Higher urban peak storm flows and Lane's Balance may explain the trend in S, while the trend in VC is hard to explain via urban changes to hydrology. The trends in K with change in total percent impervious follow the total impervious trends, indicating that new construction also plays a role. At the reach level, increased forested buffer width (i.e. decreased urbanization in the riparian zone) is associated with essentially no change in any hyporheic potential metric, due either to conflicting processes or more general lack of influence at the reach scale.

Despite the noisiness inherent in this type of study, the weak correlations lead to the following general conclusions. First, controls on hyporheic potential are scale dependent, with

watershed-level processes being more important than reach-level processes. Both reach-level and watershed-level urbanization appear to have negligible effect on *K*, perhaps because bank erosion and streambed coarsening balance each other. Second, urbanization enhances hyporheic potential at the watershed level and (given no net effect at the reach-level) more generally. This is unexpected in that hyporheic exchange is generally considered as positive for stream ecosystems as well as humans via ecosystem services, and we generally expect urbanization to degrade stream ecosystem function. Lastly, due to the highly complex relationship between urban streams and their watersheds, a great number of processes and variables that affect urban streams can contribute heavily to the scatter observed in our results (Clapcott et al., 2010). Some of these are the bedrock geology, discharge, the use of total impervious instead of connected impervious, weather fluctuations, and the variation among watersheds in terms of storm water infrastructure.

References

Allen, J. D., Erickson, D. L., & Fay, J. (1997). The influence of catchment land use on stream integrity across multiple spatial scales. *Freshwater Biology, 37*, 149–161.

Allmendinger, N. E., Pizzuto, J. E., Potter, N. J., Johnson, T. E., & Hession, W. C. (2005). The influence of riparian vegetation on stream width, eastern Pennsylvania, USA. *GSA Bulletin, 117*, 229-243.

Banham, R. (2009). *The Fight of Fairfax: A Struggle for a Great American County.* Fairfax: GMU Press.

Bernhardt, E. S., Palmer, M. A., Allan, J. D., Alexander, G., Barnas, K., Brooks, S., et al. (2005). Synthesizing U.S. River Restoration Efforts. *Science, 308*, 636-637.

Boano, F., Camporeale, C., Revelli, R., & Ridolfi, L. (2006). Sinuosity-driven hyporheic exchange in meandering rivers. *Geophysical Research Letters, 33*, L18406.

Booth, D. B., & Jackson, C. R. (1997). Urbanization of Aquatic Systems: DegradationThresholds, Stormwater Detection, and the Limits of Mitigation. *Journal of the American Water Resources Association, 33* (5), 1077-1090.

Booth, D. B., Hartley, D., & Jackson, R. (2002). Forest Cover, Impervious-Surface Area, and the Mitigation of Stormwater Impacts. *Journal of the American Water Resources Association, 38* (3), 835-845.

Booth, D. B., Karr, J. R., Schauman, S., Konrad, C. P., Morley, S. A., Larson, M. G., et al. (2004). Reviving Urban Streams: Land Use, Hydrology, Biology, and Human Behavior. *Journal of the American Water Resources Association*, 1351-1364.

Boulton, A. J. (2007). Hyporheic rehabilitation in rivers: restoring vertical connectivity. *Freshwater Biology, 52*, 632–650.

Boulton, A. J., Findlay, S., Marmonier, P., Stanley, E. H., & Valett, H. M. (1998). The functional significance of the hyporheic zone in streams and rivers. *Annual Review of Ecology and Systematics, 29*, 59-81.

Brabec, E., Schulte, S., & Richards, P. L. (2002). Impervious Surfaces and Water Quality: A Review of Current Literature and Its Implications for Watershed Planning. *Journal of Planning Literature, 16* (4), 499-514.

Briggs, M. A., Gooseff, M. N., Peterson, B. J., Morkeski, K., Wollheim, W. M., & Hopkinson, C. S. (2010). Surface and hyporheic transient storage dynamics throughout a coastal stream network. *Water Resources Research, 46*.

Brunke, M. (1999). Colmation and Depth Filtration within Streambeds: Retention of Particles in Hyporheic Interstices. *International Review of Hydrobiology, 84* (2), 99-117.

Brunke, M., & Gonser, T. (1997). The ecological significance of exchange processes between rivers and groundwater. *Freshwater Biology, 33*, 1-33.

Calver, A. (2001). Riverbed Permeabilities: Information from Pooled Data. *Ground Water*, *39* (4), 546-553.

Cardenas, M. B. (2009). A model for lateral hyporheic flow based on valley slope and channel sinuosity. *Water Resources Research, 45*, W01501.

Carter, J., Owens, P. N., Walling, D. E., & Leeks, G. J. (2003). Fingerprinting suspended sediment sources in a large urban river system. *The Science of the Total Environment, 314-316*, 513–534.

Chen, X. (2000). Measurement of streambed hydraulic conductivity and its anisotropy. *Environmental Geology, 39* (12), 1317-1324.

Chen, X., Zhang, Z., Chen, X., & Shi, P. (2009). The impact of land use and land cover changes on soil moisture and hydraulic conductivity along the karst hillslopes of southwest China. *Environmental Earth Sciences, 59*, 811-820.

Chin, A. (2006). Urban transformation of river landscapes in a global context. *Geomorphology, 79*, 460-487.

Cianfrani, C. M., Hession, W. C., & Rizzo, D. M. (2006). Watershed Imperviousness Impacts on Stream Channel Condition in Southeastern Pennsyvania. *Journal of the American Water Resources Association*, 941-956.

Clapcott, J. E., Young, R. G., Goodwin, E. O., & Leathwick, J. R. (2010). Exploring the response of functional indicators of stream health to land-use gradients. *Freshwater Biology, 55*, 2181–2199.

Colosimo, M. F., & Wilcock, P. R. (2007). Alluvial Sedimentaion and Erosion in an Urbanizing Watershed, Gwynns Falls, Maryland. *Journal of the American Water Resources Association, 43* (2), 499-521.

Conant, B., Cherry, J. A., & Gillham, R. W. (2004). A PCE groundwater plume discharging to a river: influence of the streambed and near-river zone on contaminant distributions. *Journal of Contaminant Hydrology, 73*, 249-279.

Cranmer, E. (2009). *Stratigraphic Reconstruction of Holocene Paleogeography and Paleoclimate, Little Falls, MD.* Undergraduate Honors Thesis, Franklin & Marshall College, Earth & Environment.

Cranmer, M. (2010). (Pers. Com., May 29, 2010).

Cuffney, T. F., Brightbill, R. A., May, J. T., & Waite, I. R. (2010). Responses of benthic macroinvertebrates to environmental changes associated with urbanization in nine metropolitan areas. *Ecological Applications, 20* (5), 1384-1401.

Dent, C. L., Schade, J. D., Grimm, N. B., & Fisher, S. G. (2000). Subsurface influences on surface biology. In J. B. Jones, & P. J. Mulholland (Eds.), *Streams and groundwaters* (pp. 281-402). San Diego: Academic Press.

Doyle, M. W., Harbor, J. M., Rich, C. F., & Spacie, A. (2000). Examining the Effects of Urbanization on Streams Using Indicators of Geomorphic Stability. *Physical Geography, 21* (2), 155-181.

Fischer, H., Kloep, F., Wilzcek, S., & Pusch, M. T. (2005). A river's liver - microbial processes within the hyporheic zone of a large lowland river. *Biogeochemistry, 76*, 349-371.

Fries, J. S., & Taghon, G. L. (2010). Particle Fluxes into Permeable Sediments: Comparison of Mechanisms Mediating Deposition. *Journal of Hydraulic Engineering*, 214-221.

Fry, J. A., Coan, M. J., Homer, C. G., Meyer, D. K., & Wickham, J. D. (2009). *Completion of the National Land Cover Database (NLCD) 1992–2001 Land Cover Change Retrofit product.* U.S. Geological Survey Open-File Report 2008–1379.

Fullerton, A. H., Beechie, T. J., Baker, S. E., Hall, J. E., & Barnas, K. A. (2006). Regional patterns of riparian characteristics in the interior Columbia River basin, Northwestern USA: applications for restoration planning. *Landscape Ecology, 21*, 1347–1360.

Galster, J. C., Pazzaglia, F. J., Hargreaves, B. R., Morris, D. P., Peters, S. C., & Weisman, R. N. (2006). Effects of urbanization on watershed hydrology: The scaling of discharge with drainage area. *Geology, 34* (9), 713-716.

Gandy, C. J., Smith, J. W., & Jarvis., A. P. (2007). Attenuation of mining-derived pollutants in the hyporheic zone: A review. *Science of the Total Environment, 373*, 435-446.

Genereux, D. P., Leahy, S., Mitasova, H., Kennedy, C. D., & Corbett, D. R. (2008). Spatial and temporal variability of streambed hydraulic conductivity in West Bear Creek, North Carolina, USA. *Journal of Hydrology, 358*, 332-353.

Gooseff, M. N., Anderson, J. K., Wondzell, S. M., LaNier, J., & Haggerty, R. (2006). A modeling study of hyporheic exchange pattern and the sequence, size, and spacing of stream bedforms in mountain stream networks, Oregon, USA. *Hydrological Processes, 20*, 2443-2457.

Gooseff, M. N., Hall Jr., R. O., & Tank, J. L. (2007). Relating transient storage to channel complexity in streams of varying land use in Jackson Hole, Wyoming. *Water Resources Research, 43*, W01417.

Graf, W. L. (1975). The Impact of Suburbanization on Fluvial Geomorphology. *Water Resources Research, 11* (5), 690-692.

Gran, K., & Paola, C. (2001). Riparian vegetation controls on braided stream dynamics. *Water Resources Research, 37* (12), 3275-3283.

Groffman, P. M., Dorsey, A. M., & Mayer, P. M. (2005). N processing within geomorphic strucutre in urban streams. *Journal of the North American Benthological Societ , 24*, 613-625.

Hancock, P. J. (2002). Human impacts on the stream-groundwater exchange zone. *Environmental Management, 29* (6), 763-781.

Harvey, J. W., & Bencala, K. E. (1993). The Effect of Streambed Topography on Surface-Subsurface Water Exchange in Mountain Catchments. *Water Resources Research, 29* (1), 89-98.

Hester, E. T., & Doyle, M. W. (2008). In-stream geomorphic structures as drivers of hyporheic exchange. *Water Resources Research, 44*, W03417.

Hester, E., & Gooseff, M. (2010). Moving Beyond the Banks: Hyporheic Restoration Is Fundamental to Restoring Ecological Services and Functions of Streams. *Environmental Science & Technology, 44* (5), 1521-1525.

Hogan, D. N., & Walbridge, M. R. (2009). Recent Land Cover History and Nutrient Retention in Riparian Wetlands. *Environmental Management, 44* (1), 62-72.

Homer, C., Huang, C., Yang, L., Wylie, B., & Coan, M. (2004). Development of a 2001 National Landcover Database for the United States. *Photogrammetric Engineering and Remote Sensing, 70* (7), 829-840.

Horslev, M. J. (1951). *Time Lag and Soil Permeability in Groundwater Observations.* Vicksburg, Mississippi: US Army Bulletin 36, US Army Corps of Engineers, Waterways Experiment Station.

Horwitz, R. J., Johnson, T. E., Overbeck, P. F., O'Donnell, T. K., Hession, W. C., & Sweeney, B. W. (2008). Effects of Riparian Vegetation and Watershed Urbanization on Fishes in Streams of the Mid-Atlantic Piedmont (USA). *Journal of the American Water Resouces Association, 44* (3), 724-741.

Jones, J. B., & Mulholland, P. J. (Eds.). (2000). *Streams and Ground Waters.* San Diego, CA: Academic Press.

Kalbus, E., Reinstorf, F., & Schirmer, M. (2006). Measuring methods for groundwater – surface water interactions: a review. *Hydrology and Earth System Sciences, 10*, 873–887.

Kang, R. S., & Marston, R. A. (2006). Geomorphic effects of rural-to-urban land use conversion on three streams in the Central Redbed Plains of Oklahoma. *Geomorphology, 79*, 488-506.

Kasahara, T., & Hill, A. R. (2008). Modeling the effects of lowland stream restoration projects on stream–subsurface water exchange. *Ecological Engineering, 32*, 310-219.

Kasahara, T., Datry, T., Mutz, M., & Boulton, A. J. (2009). Treating causes not symptoms: restoration of surface–groundwater interactions in rivers. *Marine and Freshwater Research, 60*, 976–981.

Kenwick, R. A., Shammin, M. R., & Sullivan, W. C. (2009). Preferences for riparian buffers. *Landscape and Urban Planning, 91*, 88-96.

Knighton, D. (1998). *Fluvial Forms & Processes: A New Perspective.* London: Arnold.

Landon, M. K., Rus, D. L., & Harvey, F. E. (2001). Comparison of Instream Methods for Measuring Hydraulic Conductivity in Sandy Streambeds. *Groundwater, 39* (6), 870-885.

Lane, E. W. (1955). Design of stable channels. *Transactions*, 1234-1279.

Leopold, L. B. (1968). *Hydrology for Urban Land Planning.* A Guidebook on the Hydrologic Effects of Urban Land Use, U.S. Geological Survey Circular 554.

Mays, L. W. (2005). *Water Resources Engineering* (2005 Edition ed.). John Wiley & Sons, Inc.

McMahon, G., & Cuffney, T. F. (2000). Quantifying Urban Intensity in Drainage Basins for Assessing Stream Ecological Conditions. *Journal of the American Water Resources Association, 36* (6), 1247-1261.

Merritts, D., Walter, R., Rahnis, M., Hartranft, J., Cox, S., Gellis, A., et al. (2011). Anthropocene streams and base-level controls from historic dams in the unglaciated mid-Atlantic region, USA. *Philosophical Transactions of the Royal Society A, 369* (1938), 976-1009.

Miller, S. O., Ritter, D. F., Kochel, R. C., & Miller, J. R. (1993). Fluvial responses to land-use changes and climatic variations within the Drury Creek watershed, southern Illinois. *Geomorphology, 6* (4), 309-329.

Montgomery, D. R., & Buffington, J. M. (1997). Channel-reach morphology in mountain drainage basins. *Geologial Society of America Bulletin, 109* (5), 596-611.

National Resources Conservation Service (NRCS). (2007). *Title 210: Engineering National Handbook – Part 654: Stream Restoration Design.* Washington, DC: US Department of Agriculture, Natural Resources Conservation Service.

NOAA Coastal Change Analysis Program. (n.d.). *Coastal Change Analysis Program Regional Land Cover*. Retrieved October 2010, from NOAA Coastal Services Center: http://www.csc.noaa.gov/digitalcoast/data/ccapregional/index.html

Nogaro, G., Mermillod-Blondin, F., Francois-Carcaillet, F., Gaudet, J.-P., Lafont, M., & Gibert, J. (2006). Invertebrate bioturbation can reduce the clogging of sediment: an experimental study using infiltration sediment columns. *Freshwater Biology , 51*, 1458-1473.

Notebaert, B., Verstraeten, G., Ward, P., Renssen, H., & Van Rompaey, A. (2011). Modeling the sensitivity of sediment and water runoff dynamics to Holocene climate and land use changes at the catchment scale. *Geomorphology, 126*, 18-31.

Packman, A. I., & MacKay, J. S. (2003). Interplay of stream-subsurface exchange, clay particle d*eposition, and streambed evolution. *Water Resources Research, 39* (4), 1097.

Palmer, M. A., Bernhardt, E. S., Allan, J. D., Lake, P. S., Alexander, G., Brooks, S., et al. (2005). Standards for ecologically successful river restoration. *Journal of Applied Ecology, 42*, 208–217.

Petts, G. E. (1988). Accumulation of Fine Sediment within Substrate Gravels along Two Regulated Rivers, UK. *Regulated Rivers: Research and Management, 2*, 141-153.

Pizzuto, J. E., Hession, W. C., & McBride, M. (2000). Comparing gravel-bed rivers in paired urban and rural catchments of southeastern Pennsylvania. *Geology, 28* (1), 79–82.

Pizzuto, J., & O'Neal, M. (2009). Increased mid-twentieth century riverbank erosion rates related to the demise of mill dams, South River, Virginia. *Geology, 37* (1), 19-22.

Pizzuto, J., O'Neal, M., & Stotts, S. (2010). On the retreat of forested, cohesive riverbanks. *Geomorphology, 116* (3-4), 341-352.

Pollen, N., & Simon, A. (2005). Estimating the mechanical effects of riparian vegetation on streambank stability using a fiber bundel model. *Water Resources Research, 41*, W07025.

Rehg, K. J., Packman, A. I., & Ren, J. (2005). Effects of suspended sediment characteristics and bed sediment transport on streambed clogging. *Hyrdological Processes, 19*, 413–427.

Richards, C., Johnson, L. B., & Host, G. E. (1996). Landscape-scale influences on stream habitats and biota. *Canadian Journal of Fisheries and Aquatic Sciences, 53 (Suppl 1)*, 295-311.

Riva-Murray, K., Riemann, R., Murdoch, P., Fischer, J. M., & Brightbill, R. (2010). Landscape characteristics affecting streams in urbanizing regions of the Delaware River Basin (New Jersey, New York, and Pennsylvania, U.S.). *Landscape Ecology, 25*, 1489–1503.

Roy, A. H., & Shuster, W. D. (2009). Assessing Impervious Surface Connectivity and Applications for Watershed Management. *Journal of the American Water Resources Association, 45* (1), 198-209.

Ryan, R. J., & Boufadel, M. C. (2007). Evaluation of streambed hydraulic conductivity heterogeneity in an urban watershed. *Stochastic Environmental Research and Risk Assessment, 21*, 309–316.

Ryan, R. J., Welty, C., & Larson, P. C. (2010). Variation in surface water–groundwater exchange with land use in an urban stream. *Journal of Hydrology* (392), 1-11.

Schenk, E. R., & Hupp, C. R. (2009). Legacy Effects of Colonial Millponds on Floodplain Sedimentation, Bank Erosion, and Channel Morphology, Mid-Atlantic, USA. *Journal of the American Water Resources Association, 45* (3), 597-606.

Schueler, T. (1994). The Importance of Imperviousness. *Watershed Protection Techniques, 1* (3), 100-111.

Smith, J., Surridge, B., Haxton, T. H., & Lerner, D. (2009). Pollutant attenuation at the groundwater–surface water interface: A classification scheme and statistical analysis using national-scale nitrate data. *Journal of Hydrology, 369*, 302-402.

Song, J., Chen, X., Cheng, C., Wang, D., & Wang, W. (2010). Variability of streambed vertical hydraulic conductivity with depth along the Elkhorn River, Nebraska, USA. *Chinese Science Bulletin, 55* (10), 992-999.

Steedman, R. J. (1988). Modification and Assessment of an Index of Biotic Integrity to Quantify Stream Quality in Southern Ontario. *Canadian Journal of Fisheries and Aquatic Sciences, 45*, 492-501.

Sutherland, R. C. (1995). Methodology for estimating the effective impervious area of urban watersheds. *Watershed Protection Techniques, 2* (1), 282-284.

Todd, D. K., & Mays, L. W. (2005). *Groundwater Hyrdology* (3rd Edition ed.). John Wiley & Sons, Inc.

Trimble, S. W. (1997). Contribution of Stream Channel Erosion to Sediment Yield from an Urbanizing Watershed. *Science , 278*, 1442-1444.

UK Environmental Agency. (2009). *The Hyporheic Handbook: A handbook on the groundwater–surface water interface and hyporheic zone for environment managers.*

Virginia Base Mapping Program (VBMP). (2007). VBMP Orthophotography - 2006/2007. Accessed on November 6, 2010.

Veličković, B. (2005). Colmation as one of the processes in interaction between the groundwater and surface water. *Architecture and Civil Engineering, 3* (2), 165 - 172.

Vogelmann, J. E., Howard, S. M., Yang, L., Larson, C. R., Wylie, B. K., & Van Driel, J. N. (2001). Completion of the 1990's National Land Cover Data Set for the conterminous United States. *Photogrammetric Engineering and Remote Sensing, 67*, 650-662.

Walsh, C. J., Roy, A. H., Feminella, J. W., Cottingham, P. D., Groffman, P. M., & Morgan, R. P. (2005). The urban stream syndrome: current knowledge and the search for a cure. *Journal of the North American Benthological Society, 24* (3), 706-723.

Walter, R. C., & Merritts, D. J. (2008). Natural Streams and the Legacy of water-Powered Mills. *Science, 319* (5861), 299-304.

Wang, L., Lyons, J., Kanehl, P., & Bannerman, R. (2001). Impacts of Urbanization on Stream Habitat and Fish Across Multiple Spatial Scales. *Environmental Management, 28* (2), 255-266.

Whitlow, J. R., & Gregory, K. J. (1989). Changes in Urban Stream Channels in Zimbabwe. *Regulated Rivers: Research and Management, 4*, 27-42.

Wolman, M. G. (1967). A cycle of sedimentation and erosion in urban river channels. *Geografiska Annaler, 49A*, 385-395.

Wolman, M. G. (1954). A method of sampling coarse river-bed material. *Transactions of the America Geophysical Union, 35* (6), 951-956.

Wood, P. J., & Armitage, P. D. (1997). Biological Effects of Fine Sediment in the Lotic Environment. *Environmental Management, 21* (2), 203-217.

Yagow, G., Hession, W. C., Wynn, T., & Bezak, B. (2008). *Developing Strategies for Urban Channel Erosion Quantification in Upland Coastal Zone Streams: Final Report.*

Appendix A: Appendix of Figures

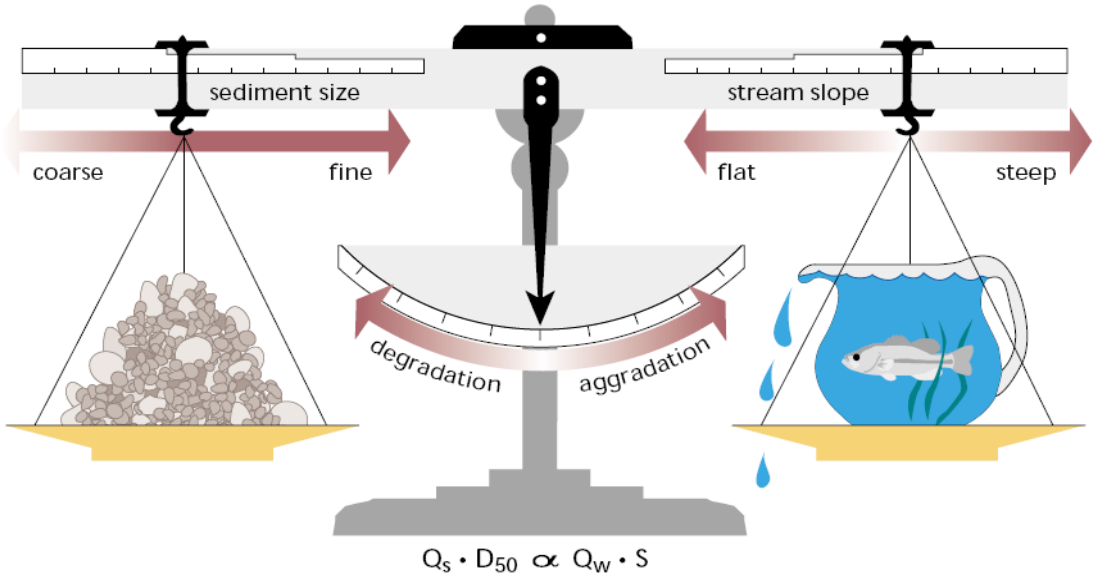

Figure 1. Lane's balance showing the relationship between sediment supply and discharge (NRCS, 2007). Used under fair use guidelines, 2011.

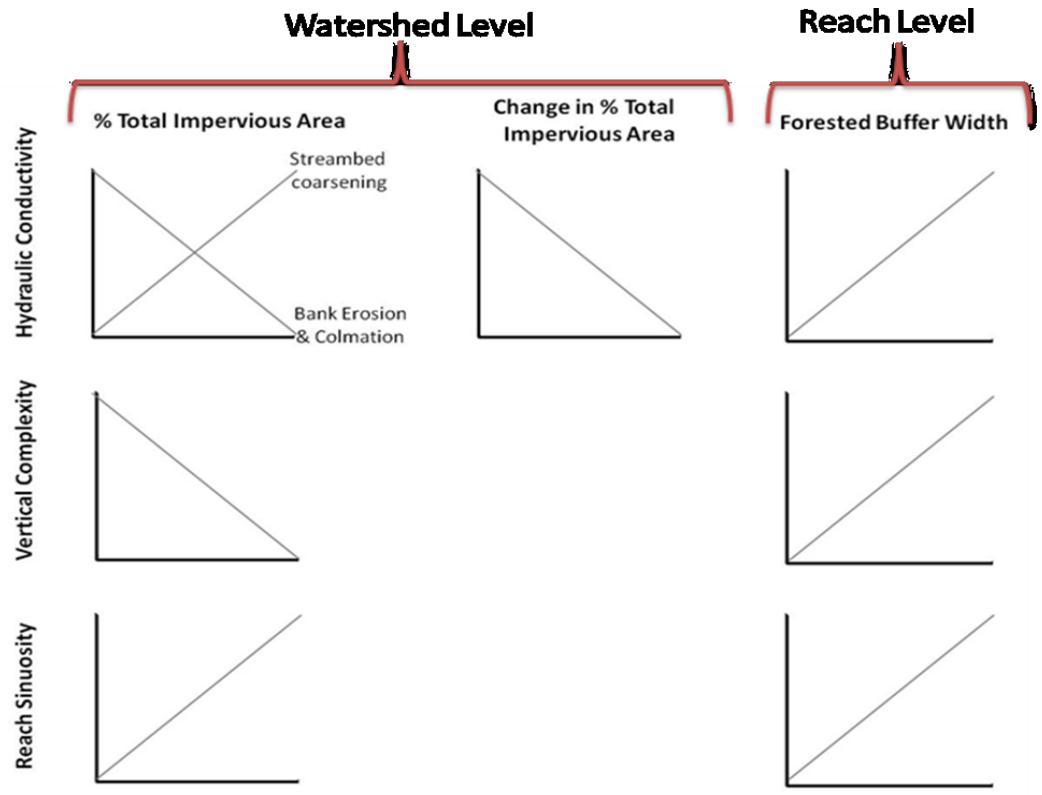

Figure 2. Expected trends of hyporheic potential with urbanization.

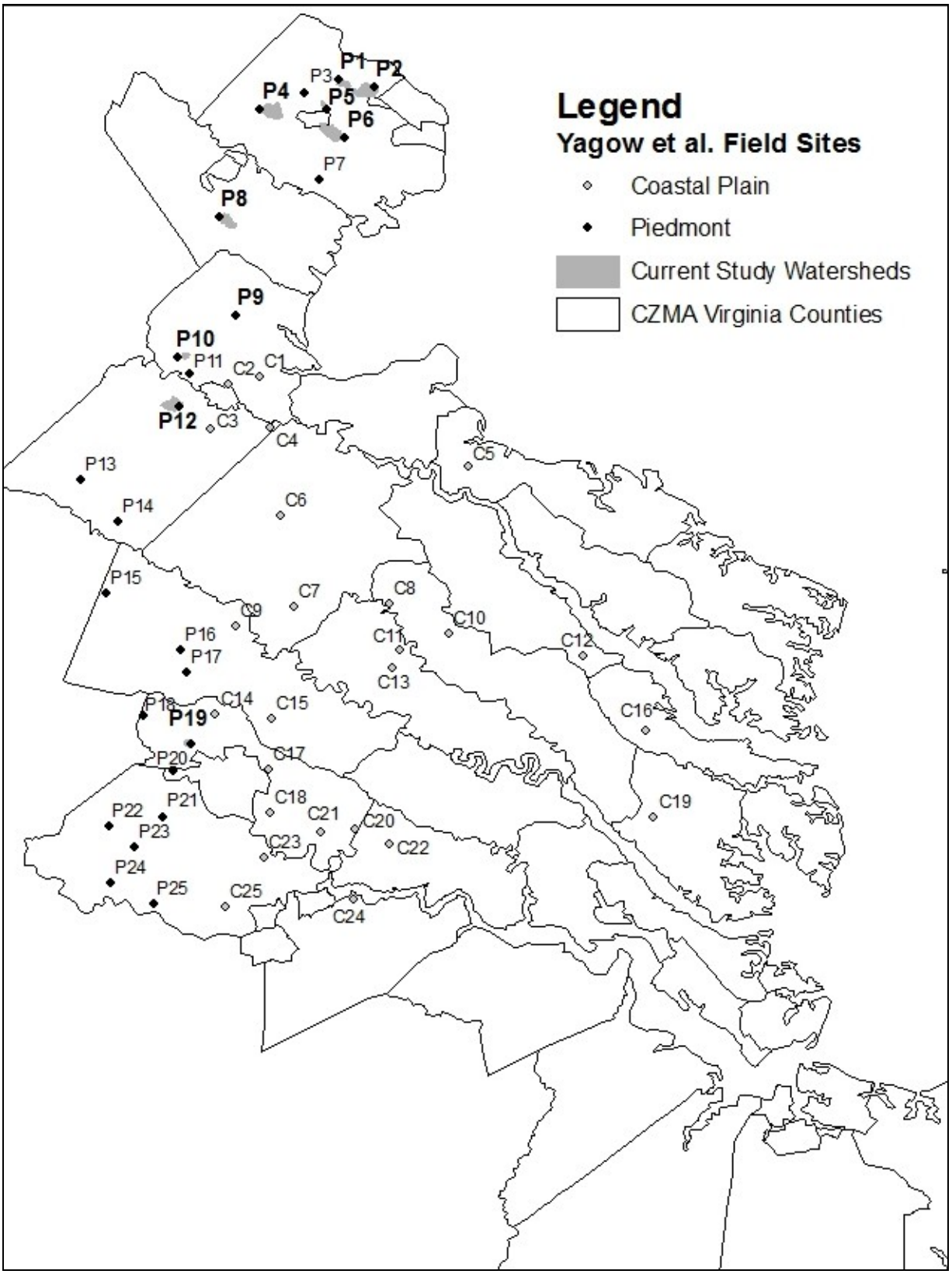

Figure 3. Field site locations from initial report by Yagow et al. (2008). Field site names for this study are bolded, while the watersheds are light grey. Used under fair use guidelines, 2011.

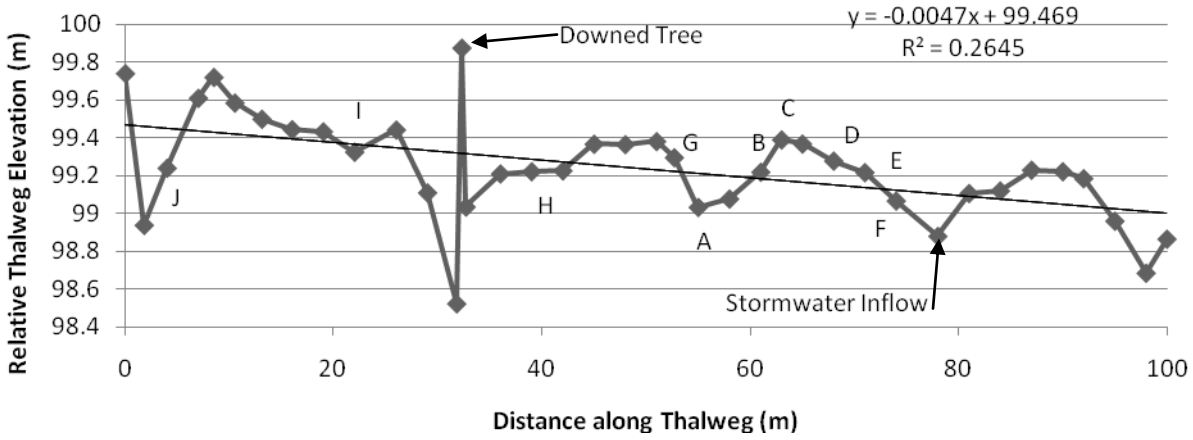

Figure 4. Thalweg survey of P1. Piezometer and permeameter locations denoted by the letters, along with pertinent features. Survey conducted in June 2010.

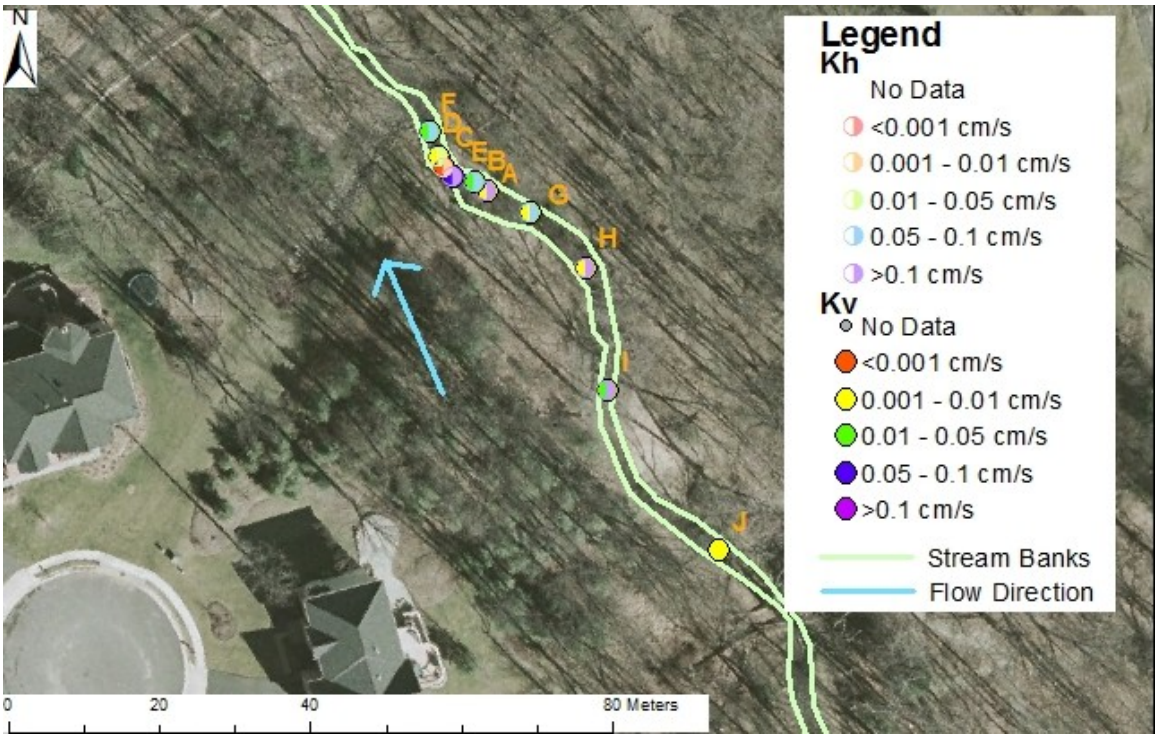

Figure 5. Digital aerial photograph of P1 showing the locations for piezometer and permeameter measurements. Aerial Imagery © 2006-2007 Commonwealth of Virginia.

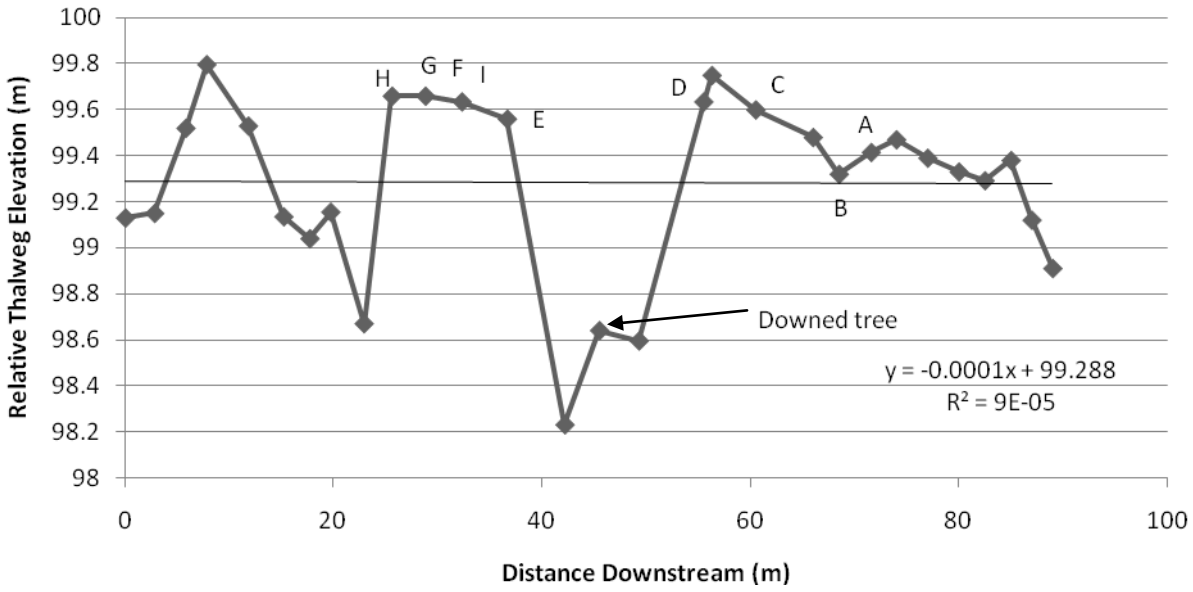

Figure 6. Thalweg survey of P2. Piezometer and permeameter locations denoted by the letters, along with pertinent features. Survey conducted in June 2010.

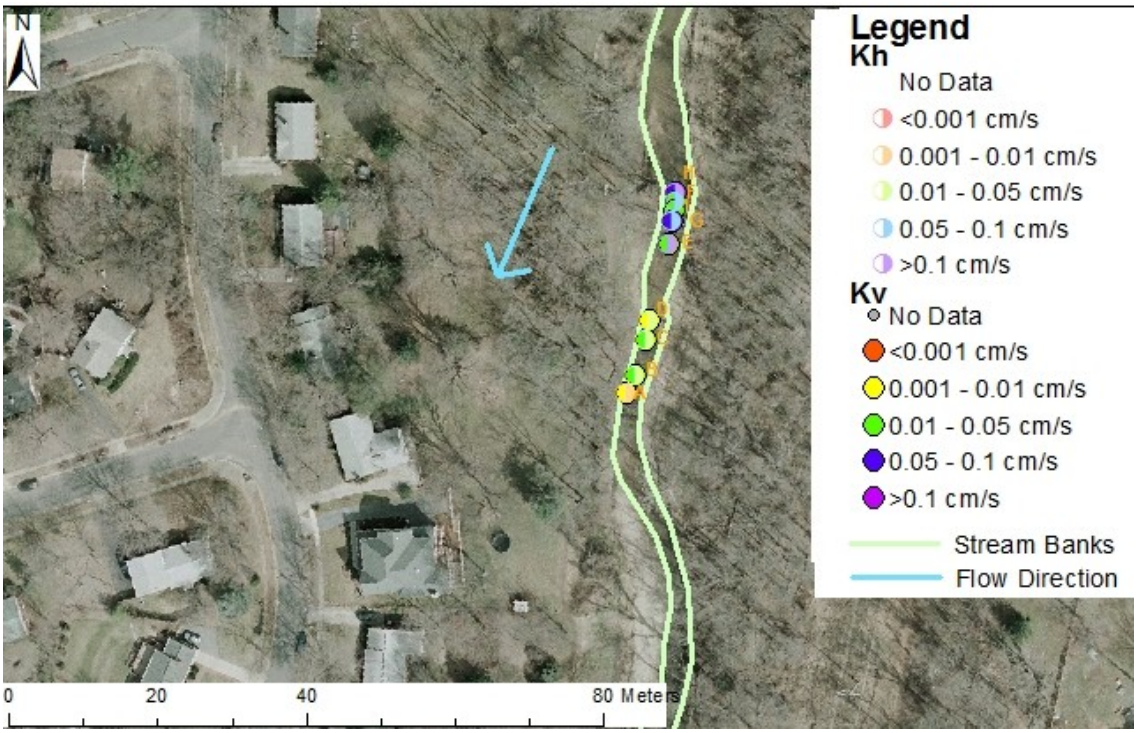

Figure 7. Digital aerial photograph of P2 showing the locations for piezometer and permeameter measurements. Aerial Imagery © 2006-2007 Commonwealth of Virginia.

Figure 8. Eroding stream bank exposing clay layer at field site P2. Photo by author, 2010.

Figure 9. Example of litter within the stream at P2. Photo by author, 2010.

Figure 10. Fallen tree disrupting stream flow at P2. Photo by author, 2010.

Figure 11. Deep pool caused by tree at field site P2. Photo by author, 2010.

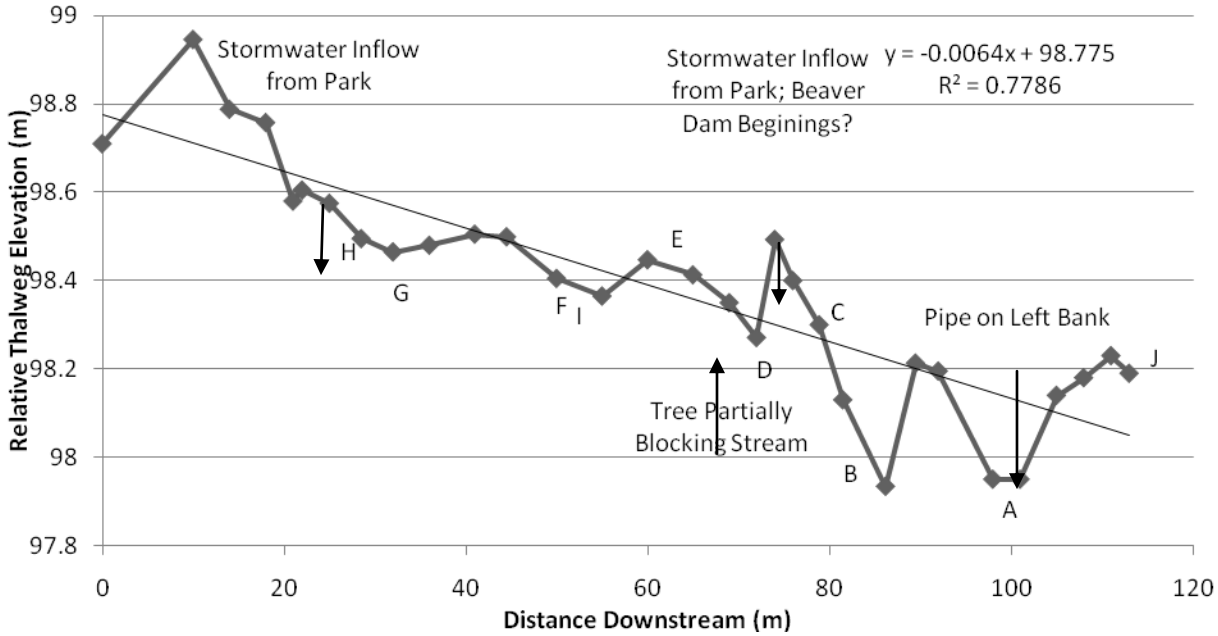

Figure 12. Thalweg survey of P4. Piezometer and permeameter locations denoted by the letters, along with pertinent features. Survey conducted in July 2010.

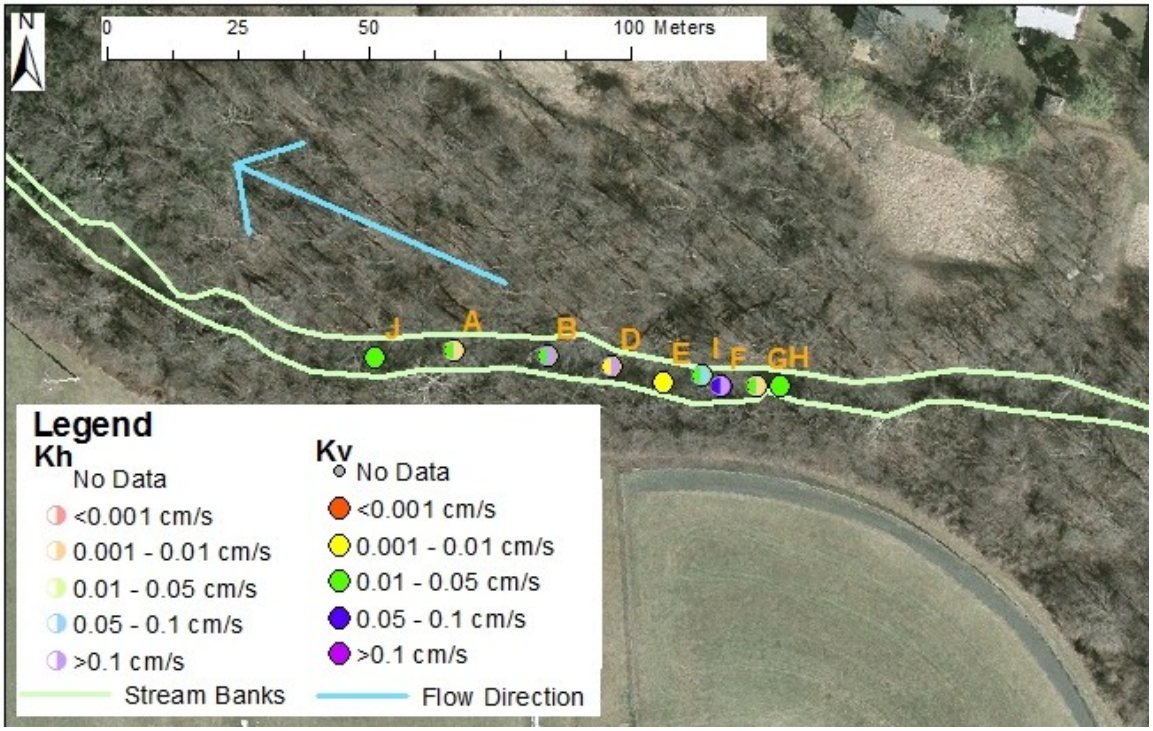

Figure 13. Digital aerial photograph of P4 showing the locations for piezometer and permeameter measurements. Aerial Imagery © 2006-2007 Commonwealth of Virginia.

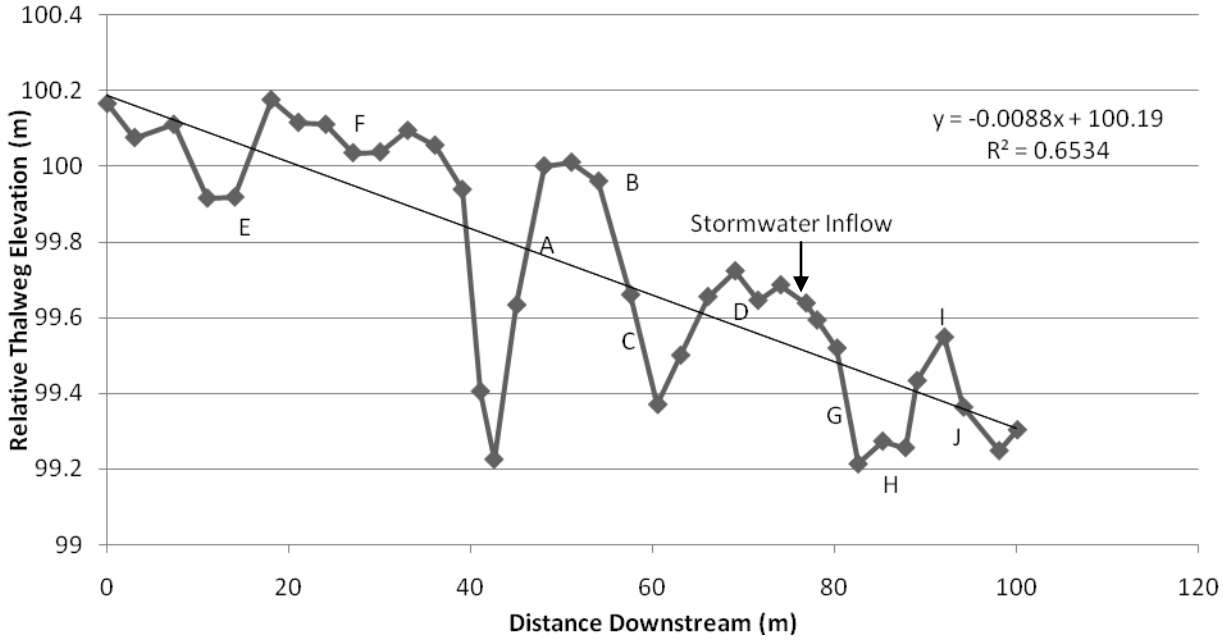

Figure 14. Thalweg survey of P5. Piezometer and permeameter locations denoted by the letters, along with pertinent features. Survey conducted in July 2010.

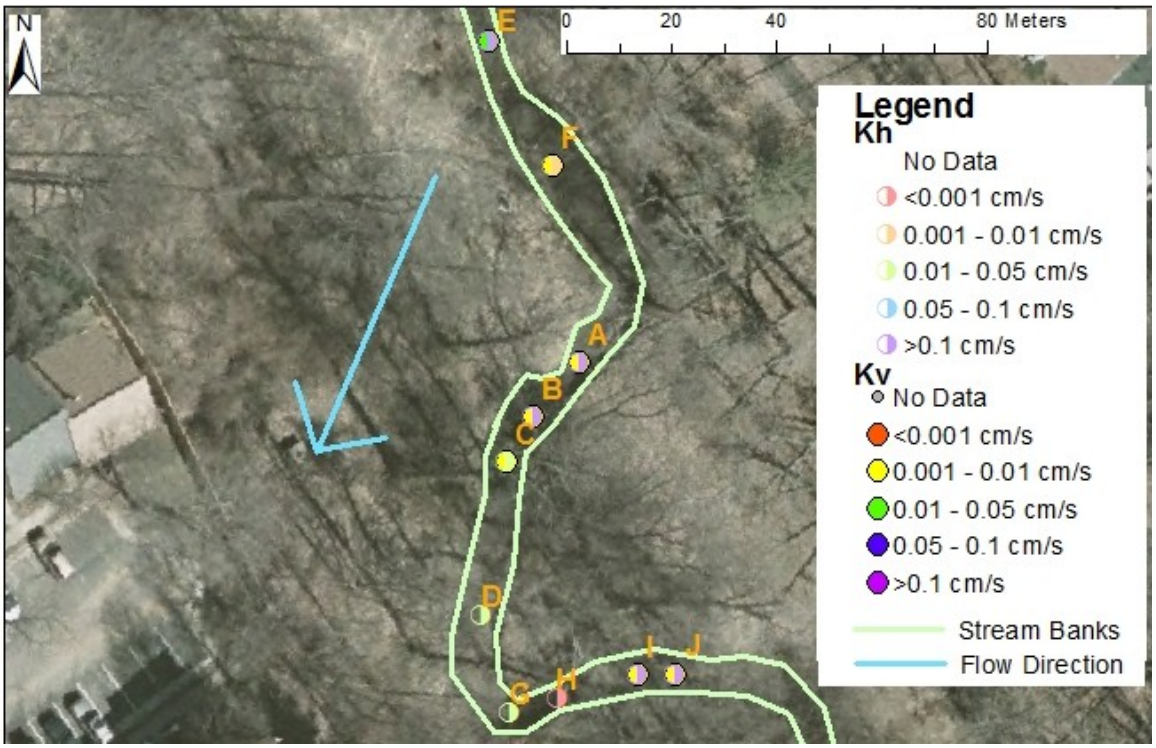

Figure 15. Digital aerial photograph of P5 showing the locations for piezometer and permeameter measurements. Aerial Imagery © 2006-2007 Commonwealth of Virginia.

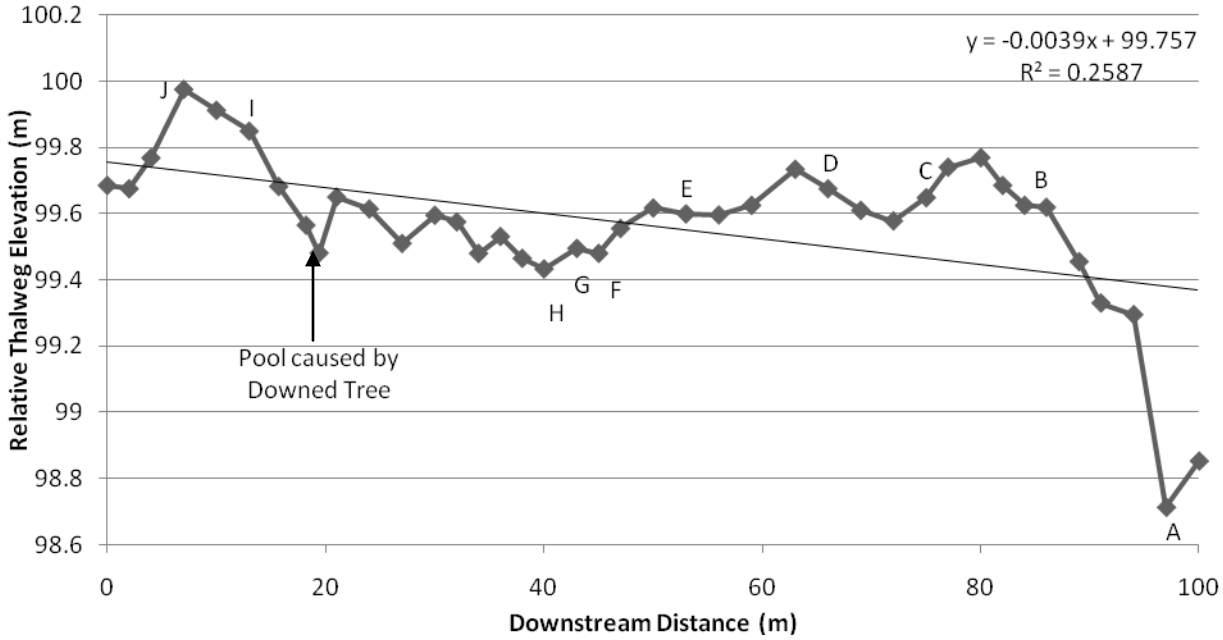

Figure 16. Thalweg survey of P6. Piezometer and permeameter locations denoted by the letters, along with pertinent features. Survey conducted in July 2010.

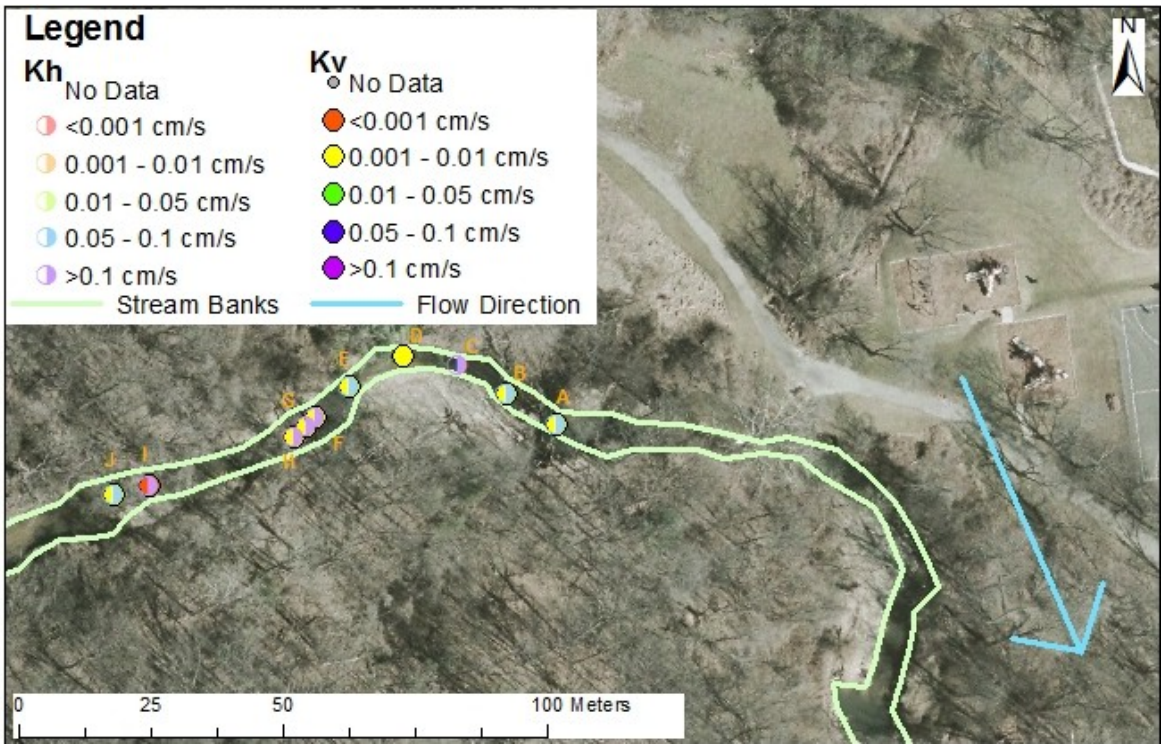

Figure 17. Digital aerial photograph of P6 showing the locations for piezometer and permeameter measurements. Aerial Imagery © 2006-2007 Commonwealth of Virginia.

Figure 18. Field photos of long pool at P6. Photo by author, 2010.

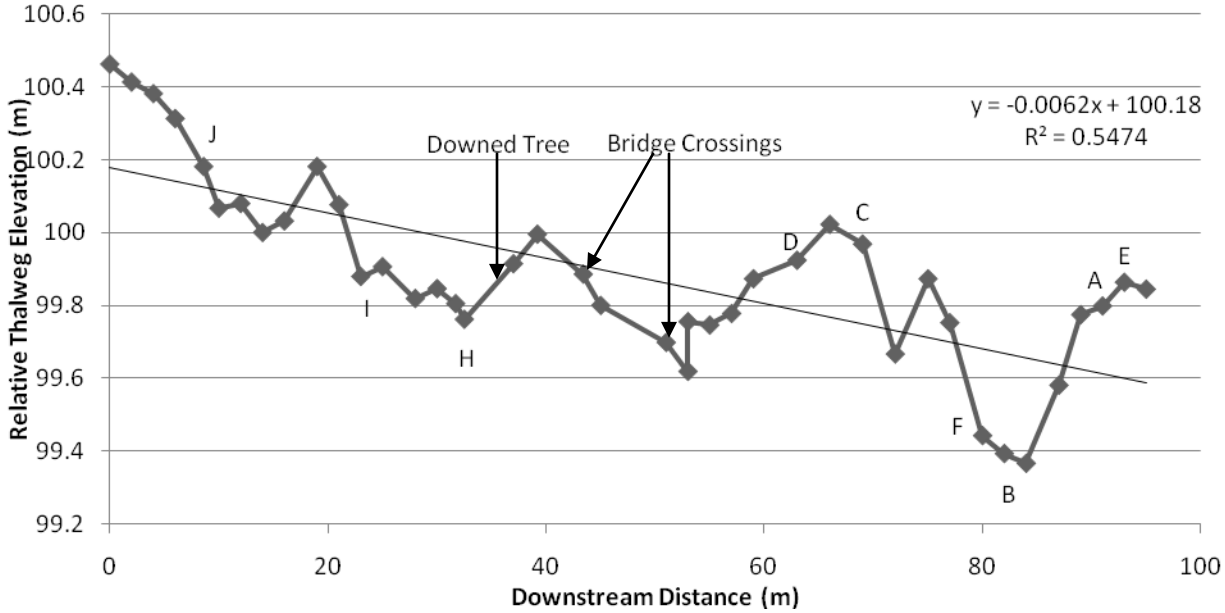

Figure 19. Thalweg survey of P8. Piezometer and permeameter locations denoted by the letters, along with pertinent features. Survey conducted in June 2010; redone in January 2011.

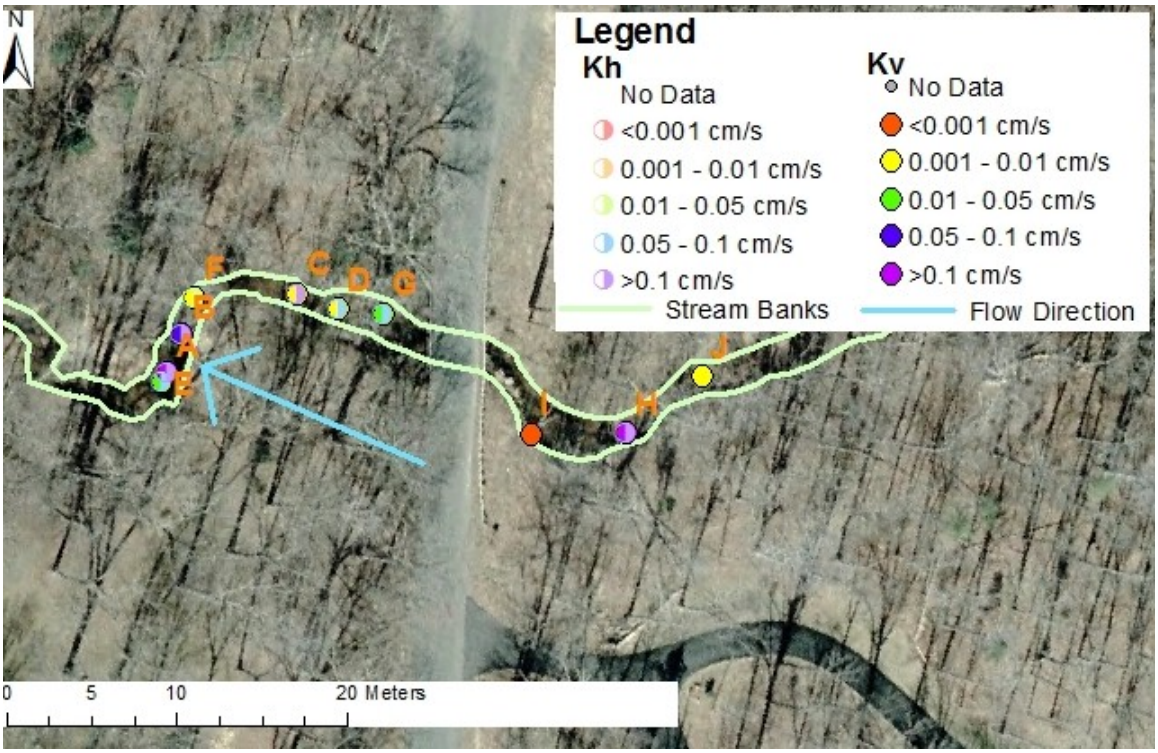

Figure 20. Digital aerial photograph of P8 showing the locations for piezometer and permeameter measurements. Aerial Imagery © 2006-2007 Commonwealth of Virginia.

Figure 21. Field photo showing the streambed at P8. Photo by author, 2010.

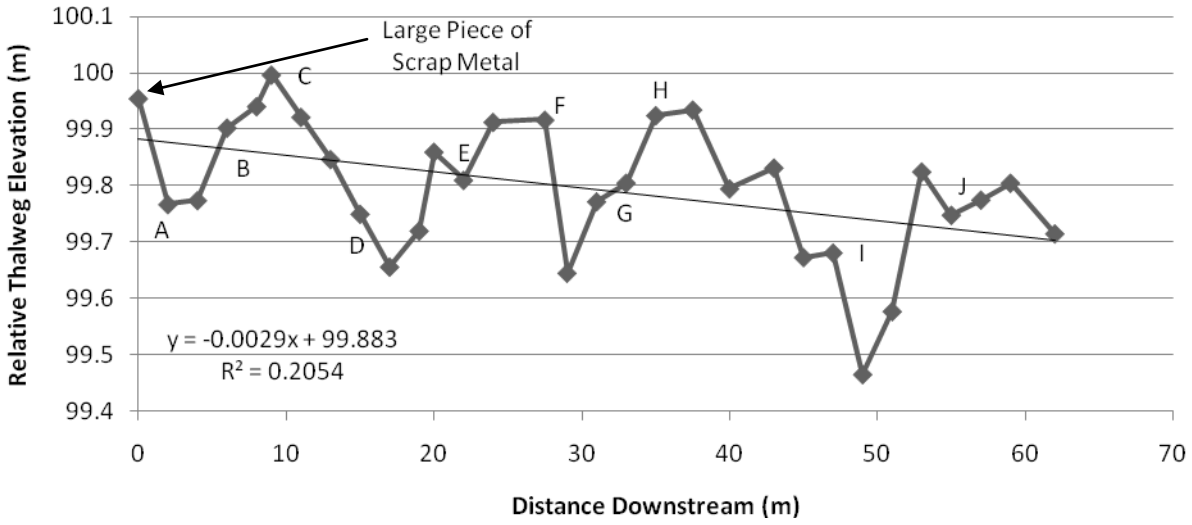

Figure 22. Thalweg survey of P9. Piezometer and permeameter locations denoted by the letters, along with pertinent features. Survey conducted in June 2010.

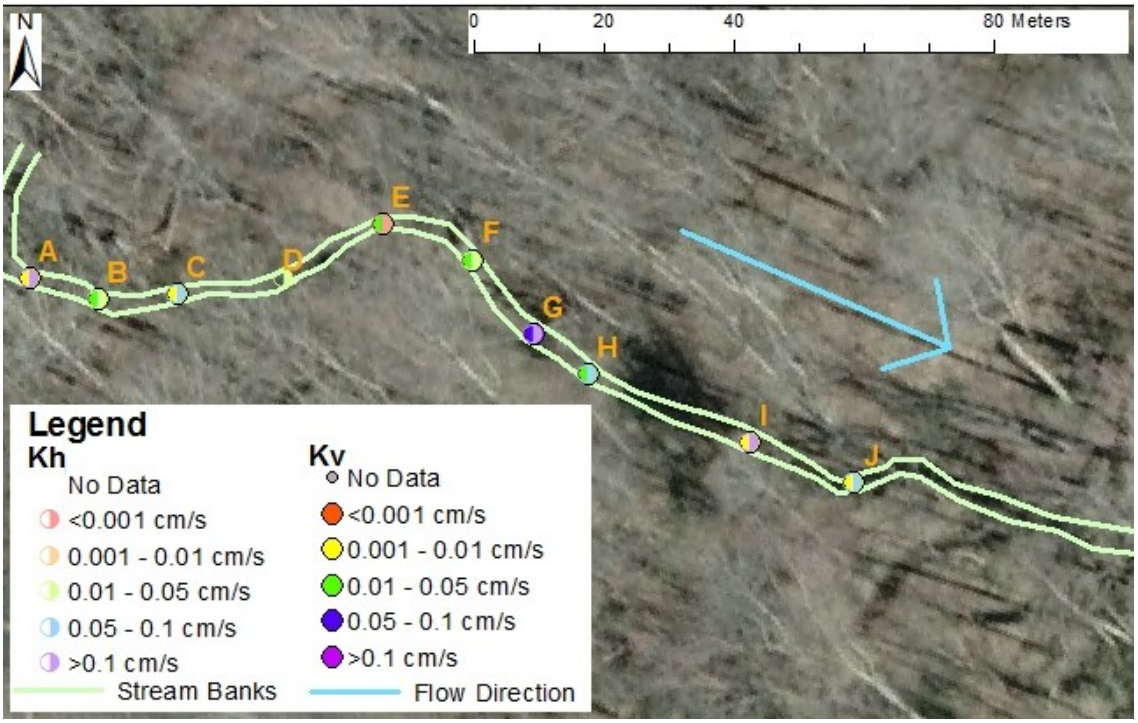

Figure 23. Digital aerial photograph of P9 showing the locations for piezometer and permeameter measurements. Aerial Imagery © 2006-2007 Commonwealth of Virginia.

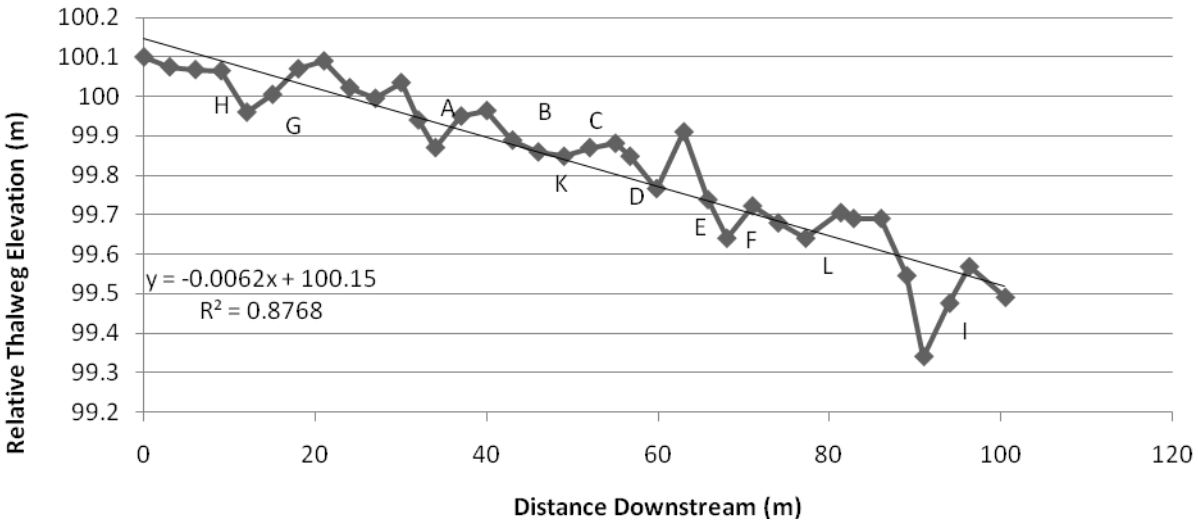

Figure 24. Thalweg survey of P10. Piezometer and permeameter locations denoted by the letters, along with pertinent features. Survey conducted in July 2010.

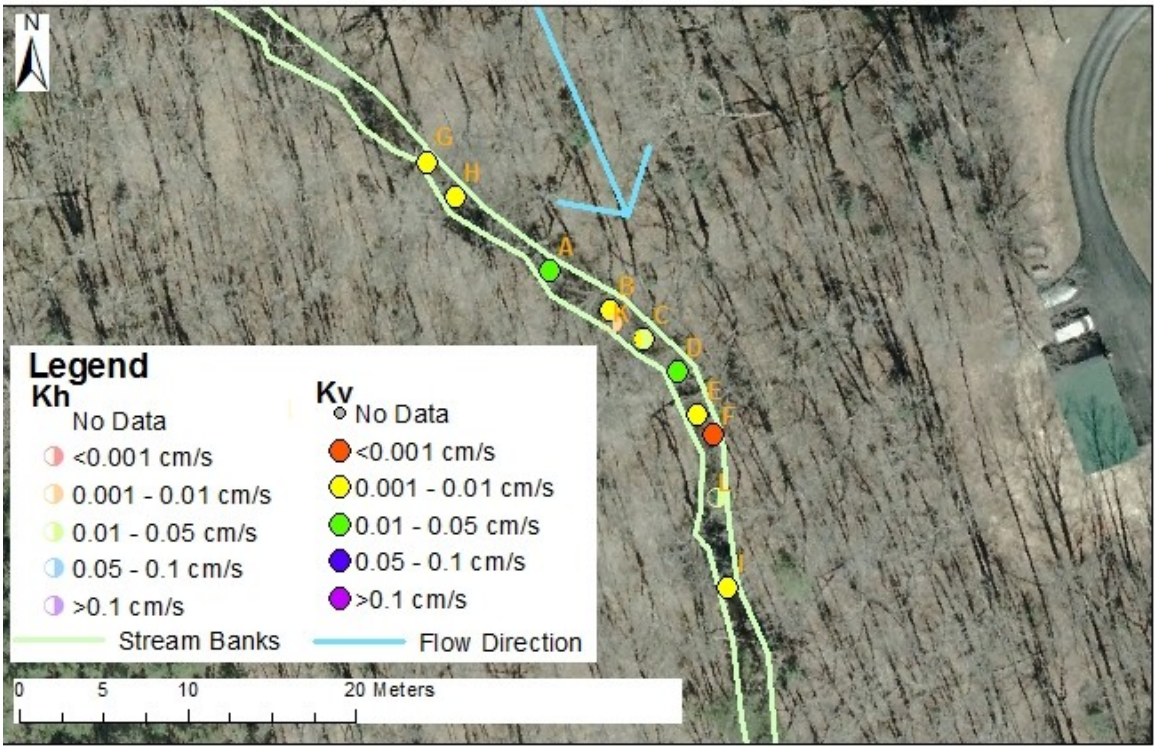

Figure 25. Digital aerial photograph of P10 showing the locations for piezometer and permeameter measurements. Aerial Imagery © 2006-2007 Commonwealth of Virginia.

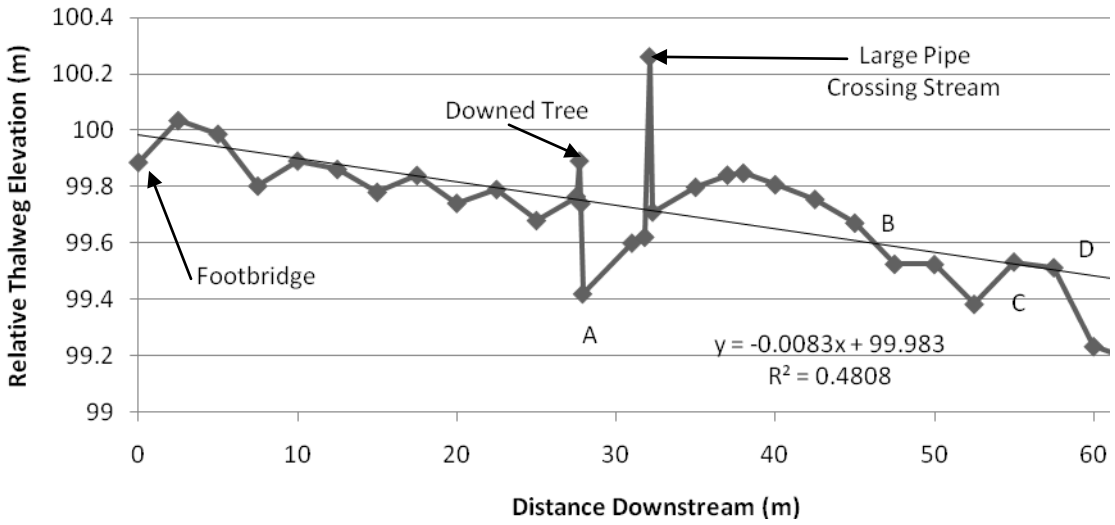

Figure 26. Thalweg survey of P12. Piezometer and permeameter locations denoted by the letters, along with pertinent features. Survey conducted in July 2010.

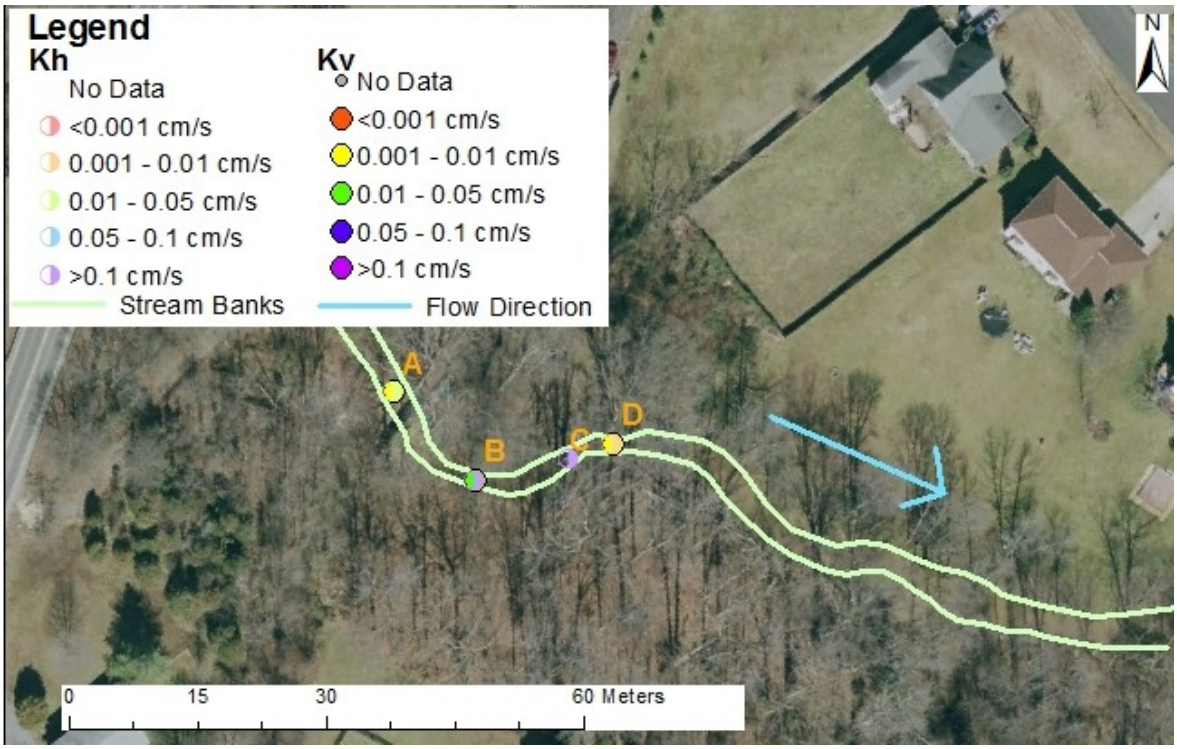

Figure 27. Digital aerial photograph of P12 showing the locations for piezometer and permeameter measurements. Aerial Imagery © 2006-2007 Commonwealth of Virginia.

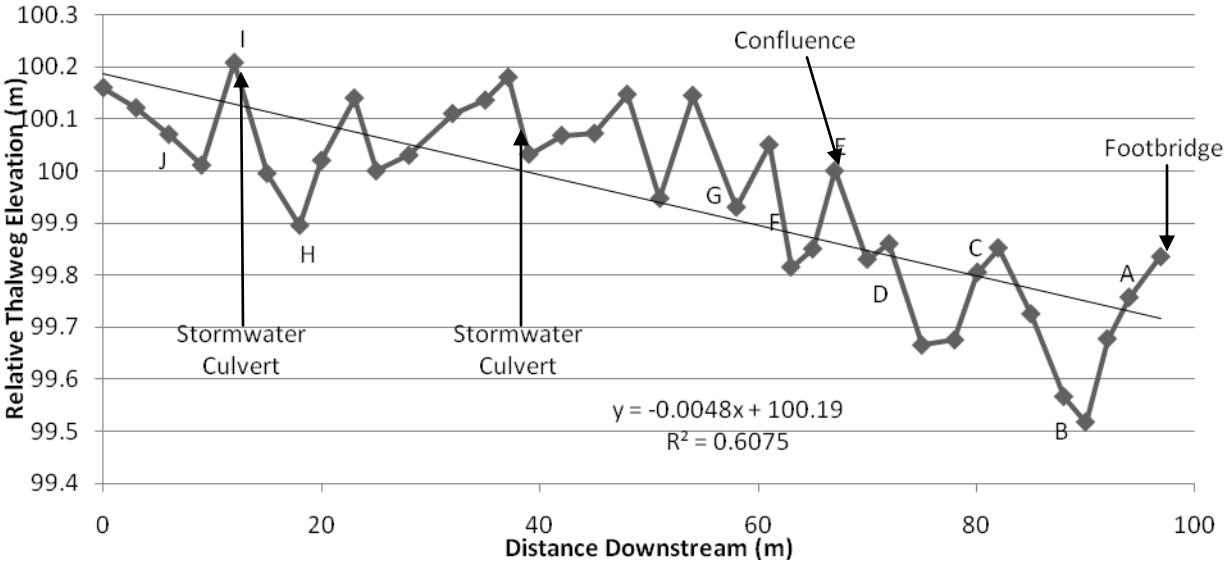

Figure 28. Thalweg survey of P19. Piezometer and permeameter locations denoted by the letters, along with pertinent features.

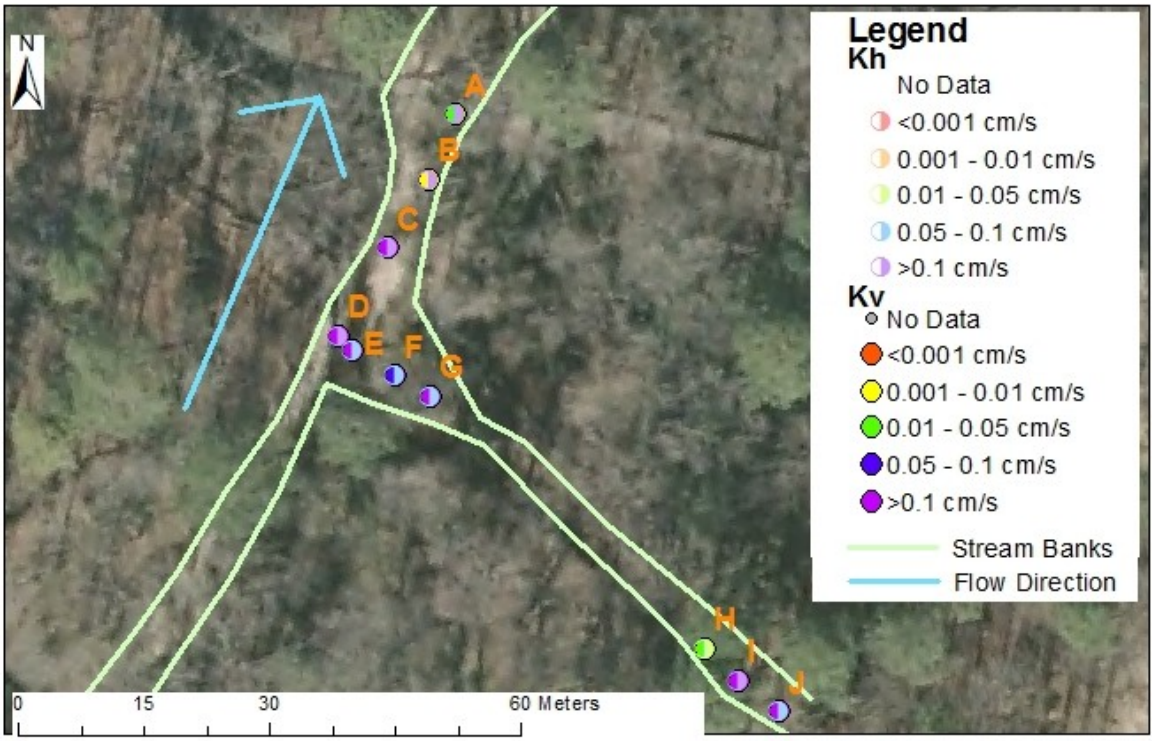

Figure 29. Digital aerial photograph of P19 showing the locations for piezometer and permeameter measurements. Aerial Imagery © 2006-2007 Commonwealth of Virginia.

Figure 30. Culverts from parking lot in P19 watershed. Photo by author, 2010.

Figure 31. Example of one of the two sewer manholes interfering with the stream in P19. Photo by author, 2010.

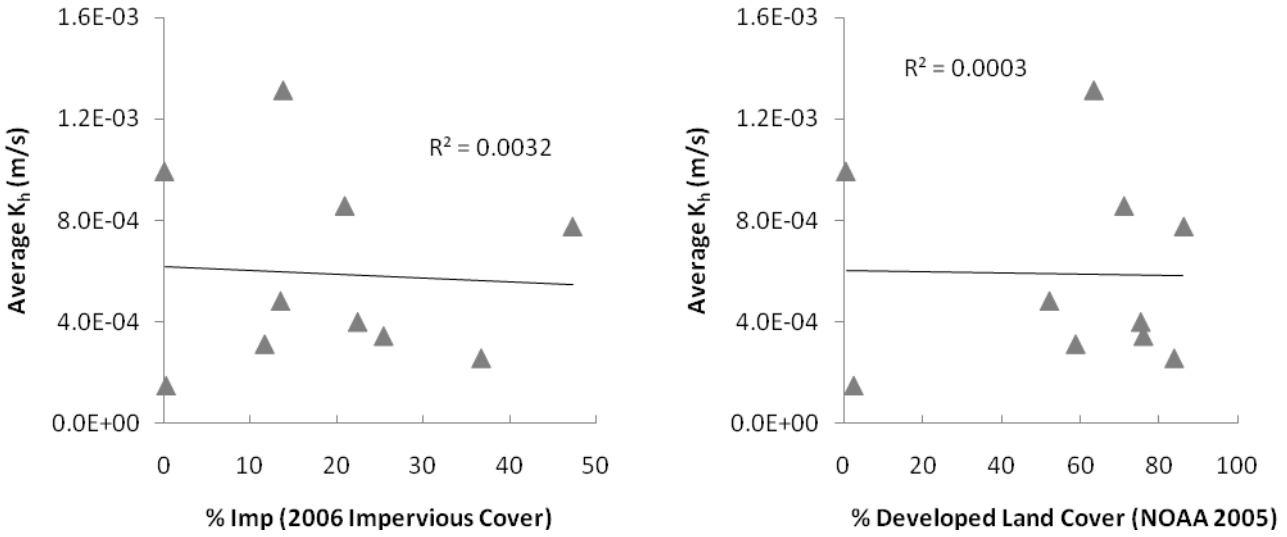

Figure 32. Horizontal hydraulic conductivity (geometric mean of the whole reach) as a function of percent impervious (2006 NLCD) and percent developed land cover (NOAA 2005).

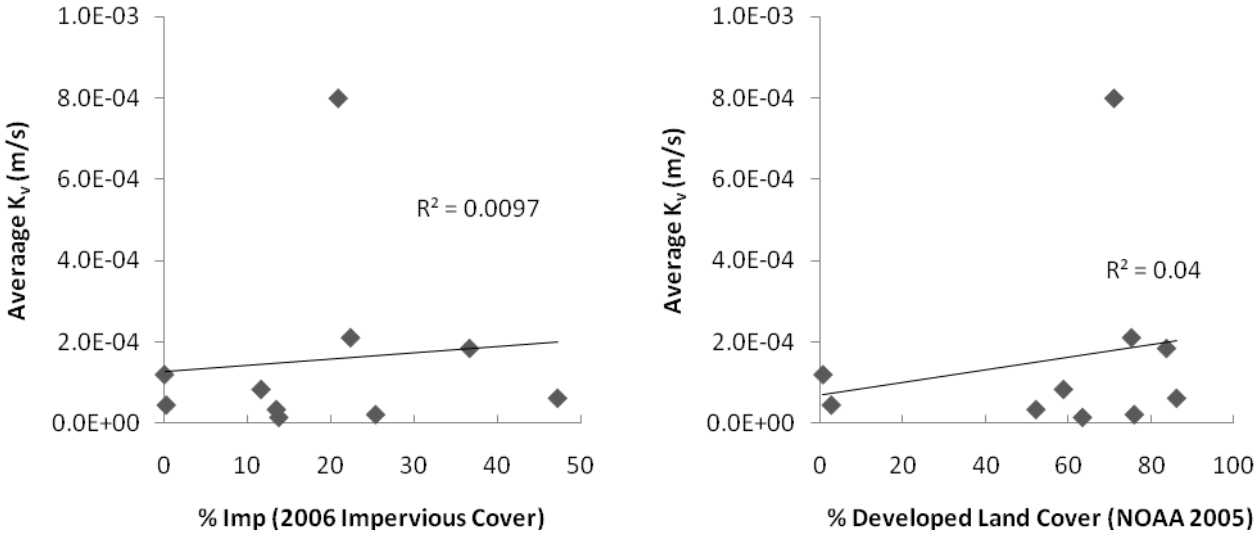

Figure 33. Vertical hydraulic conductivity (geometric mean of the whole reach) as a function of percent impervious (2006 NLCD) and percent developed land cover (NOAA 2005).

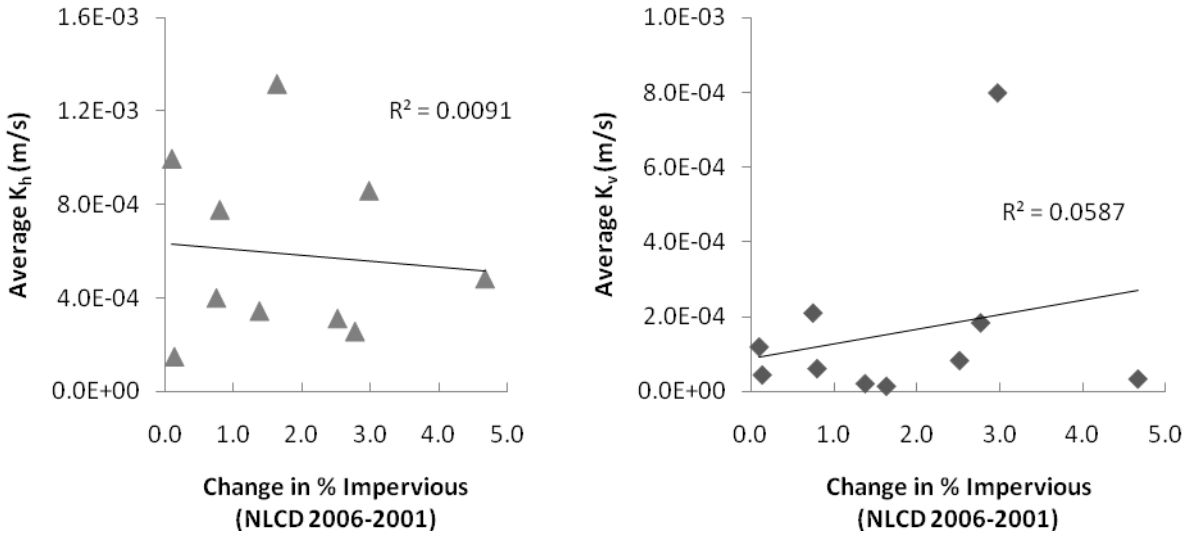

Figure 34. Hydraulic conductivity (geometric mean of whole reach) as a function of the change in percent impervious.

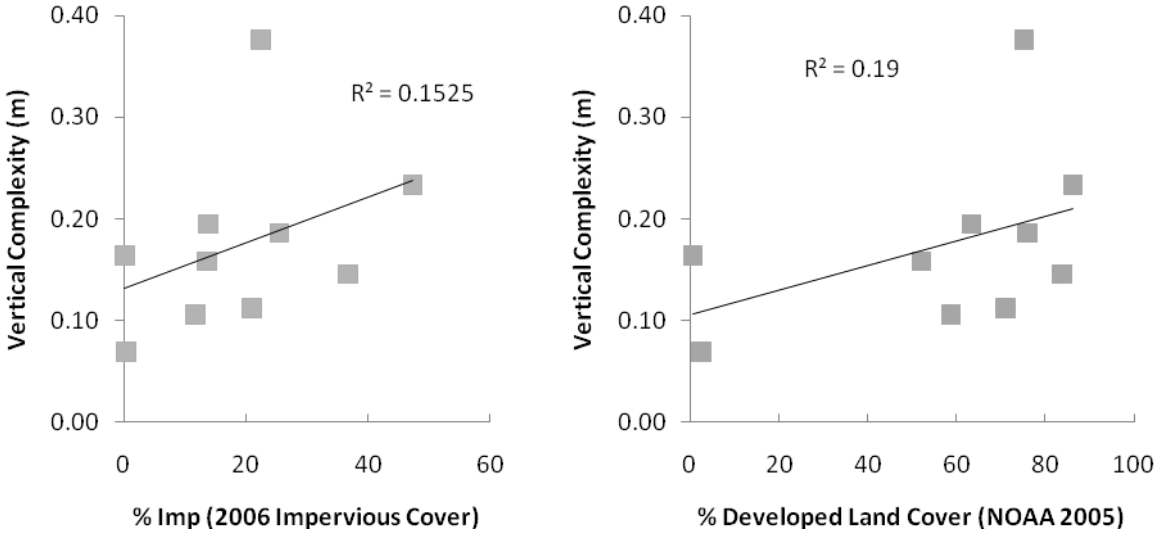

Figure 35. Vertical complexity as a function of percent developed land cover (NOAA 2005) and percent impervious (2006 NLCD).

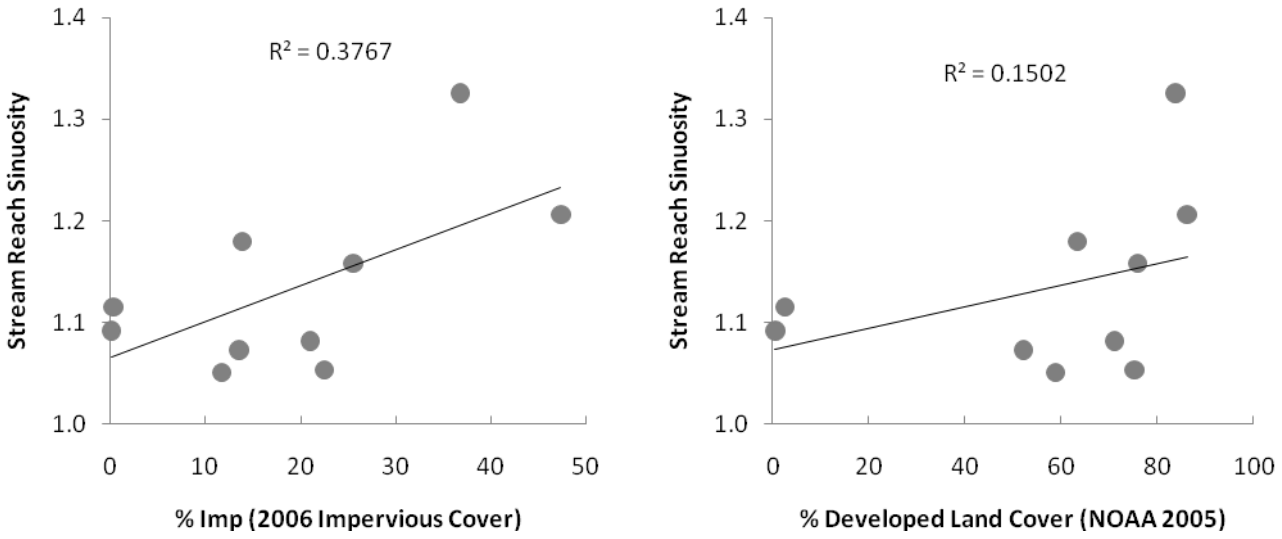

Figure 36. Sinuosity as a function of percent developed land cover (NOAA 2005) and percent impervious (2006 NLCD).

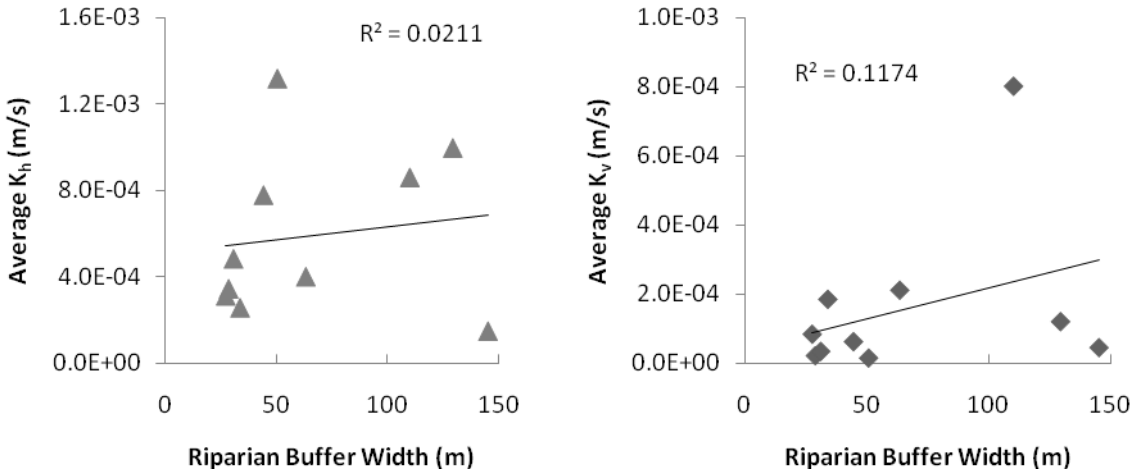

Figure 37. Hydraulic conductivity as a function of riparian buffer width.

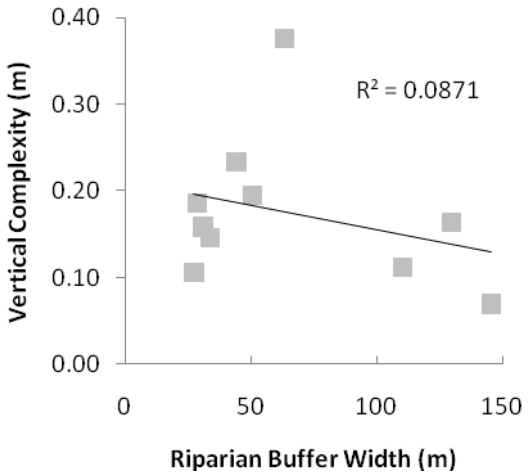

Figure 38. Vertical complexity as a function of riparian buffer width.

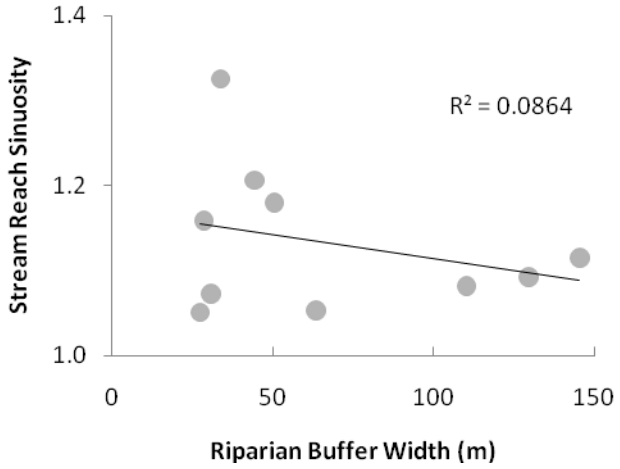

Figure 39. Local sinuosity variation with riparian buffer width.

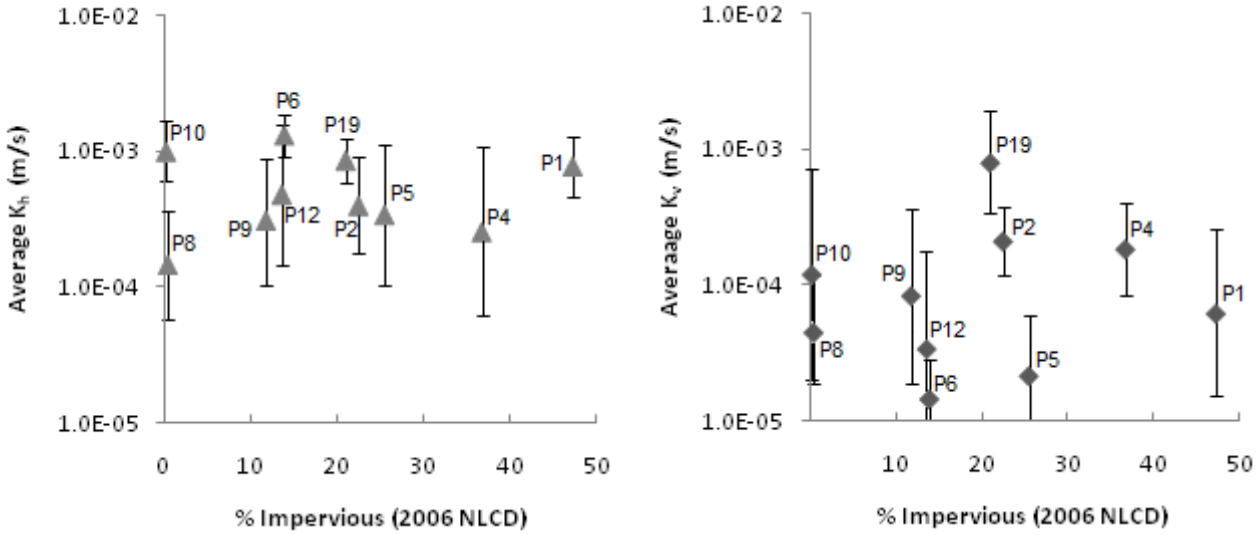

Figure 40. Horizontal hydraulic conductivity (geometric mean of the whole reach) as a function of percent impervious (2006 NLCD). The error bars are ± the standard deviation for all test locations at each stream reach site. The inherent variability within each field site causes some of the error bars to appear less than 1×10^{-5} m/s.

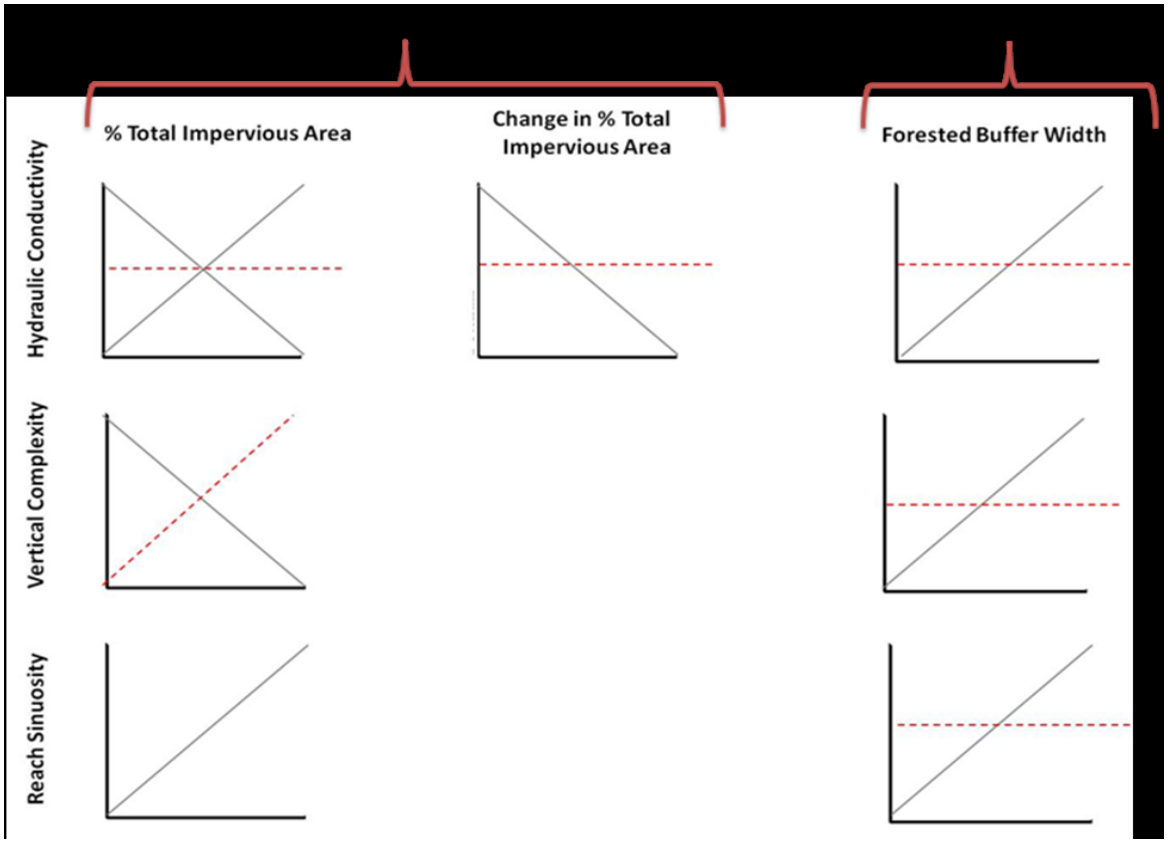

Figure 41. Summary of expected and actual hyporheic potential trends with urbanization. The coefficients of determination (r^2 values) less than 0.15 are shown as flat, while those greater to or equal 0.15 are shown as trends.

Appendix B: Appendix of Tables

Table 1. Watershed-level characteristics.

Field Site ID	Stream Name	Watershed Area (km^2)	Stream Order (NHD)	% Impervious (2006 NLCD)	% Urban Land Cover (2006 NLCD)	% Developed (2005 NOAA CSC Land Cover)	Change in % Impervious (2006-2001 NLCD)
P1	Wolftrap Creek	2.49	1	47.3	87.8	86.2	0.8
P2	----------	8.88	2	22.5	82.3	75.3	0.7
P4	Big Rocky Run	8.87	2	36.8	88.6	83.8	2.8
P5	Tributary of Accotink Creek	1.39	2	25.5	81.7	76.0	1.4
P6	Long Branch	9.47	2	13.8	68.6	63.4	1.6
P8	Tributary of Cedar Run	5.16	1	0.1	4.4	0.6	0.1
P9	----------	0.63	1	11.7	69.6	58.8	2.5
P10	Tributary of Horsepen Run	1.42	1	0.3	3.4	2.6	0.1
P12	Tributary of Northeast Creek	6.34	1	13.5	64.5	52.2	4.7
P19	Beaver Branch	1.29	1	21.0	75.9	71.1	3.0

Table 2. Reach-level characteristics

Site ID	Vertical Complexity (m)	Local Sinuosity	K_h (m/s)	Standard Deviation (m/s)	Number of Piezometers	K_v (m/s)	Standard Deviation (m/s)	Number of Permeameters	Forested Buffer Width (m)
P1	0.23	1.2	7.8E-04	5.1E-04	9	6.2E-05	2.0E-04	10	44
P2	0.38	1.1	4.0E-04	5.0E-04	8	2.1E-04	1.7E-04	8	63
P4	0.15	1.3	2.6E-04	8.4E-04	6	1.8E-04	2.1E-04	9	34
P5	0.19	1.2	3.4E-04	7.6E-04	10	2.1E-05	3.9E-05	10	29
P6	0.19	1.2	1.3E-03	5.5E-04	9	1.4E-05	1.4E-05	10	51
P8	0.16	1.1	1.0E-03	7.1E-04	8	1.2E-04	5.9E-04	10	130
P9	0.11	1.1	3.1E-04	5.6E-04	9	8.3E-05	2.8E-04	10	27
P10	0.07	1.1	1.5E-04	2.1E-04	3	4.5E-05	7.2E-05	10	145
P12	0.16	1.1	4.8E-04	1.1E-03	4	3.4E-05	1.4E-04	4	31
P19	0.11	1.1	8.6E-04	3.9E-04	10	8.0E-04	1.1E-03	10	110

Table 3. Mean hydraulic conductivity values by loosely defined geomorphic features.

	Mean K_h (m/s)			Mean K_v (m/s)		
	Pool	**Riffle**	**Run**	**Pool**	**Riffle**	**Run**
P1	9.88E-04	3.88E-04	1.05E-03	7.40E-05	5.29E-05	5.60E-05
P2		5.91E-04	1.82E-04		2.23E-04	2.51E-04
P4	2.85E-04		4.03E-04	1.05E-04	1.77E-04	2.24E-04
P5	3.52E-04	6.06E-04	1.82E-04	1.16E-05	7.06E-05	3.93E-05
P6	8.73E-04	1.10E-03	1.59E-03	1.11E-05	9.95E-06	1.80E-05
P8	5.71E-04	2.31E-03	1.08E-03	2.11E-04	1.42E-05	6.72E-04
P9	3.53E-04	6.94E-04	2.10E-04	9.47E-05	4.37E-05	1.14E-04
P10			1.48E-04	9.96E-05	5.84E-05	2.85E-05
P12	4.82E-04			3.37E-05		
P19	6.65E-04		1.02E-03	4.00E-04		1.27E-03